Electronic Supplementary Information

Endo-Functionalized Molecular Tubes: Selective Encapsulation of Neutral Molecules in Nonpolar Media

Guobao Huang,[a,c] Arto Valkonen,[b] Kari Rissanen,[b] and Wei Jiang*[a]

a Department of Chemistry, South University of Science and Technology of China(SUSTC), Shenzhen, 518055, China

**E-mail: jiangw@sustc.edu.cn*

b Department of Chemistry, Nanoscience Center, P.O. Box. 35, FI-40014 University of Jyvaskyla, Finland

c School of Chemistry and Environment, South China Normal University(SCNU), Guangzhou, 510006, China

Table of Contents

1. General Methods

All the reagents and guest molecules involved in this research were commercially available and used without further purification unless otherwise noted. Solvents were either employed as purchased or dried prior to use by standard laboratory procedures. Thin-layer chromatography (TLC) was carried out on 0.25 mm Yantai silica gel plates (60F-254). Column chromatography was performed on silica gel 60 (Tsingdao 40 – 63 nm, 230 – 400 mesh). ^{1}H, ^{13}C NMR spectra were recorded on a Bruker Avance-400 NMR spectrometer. All chemical shifts are reported in ppm with residual solvents or TMS (tetramethylsilane) as the internal standards. The following abbreviations were used for signal multiplicities: s, singlet; d, doublet; dd, doublet of doublet; m, multiplet. Electrospray-ionization high-resolution mass spectrometry (ESI-HRMS) experiments were conducted on an applied Q EXACTIVE mass spectrometry system. All the computations were performed at the Semi-Empirical PM6 level of theory by using Spartan'14 (Wavefunction, Inc.). The synthesis of diamine **A**[1] has been reported.

2. Synthetic Procedures

Compound 3

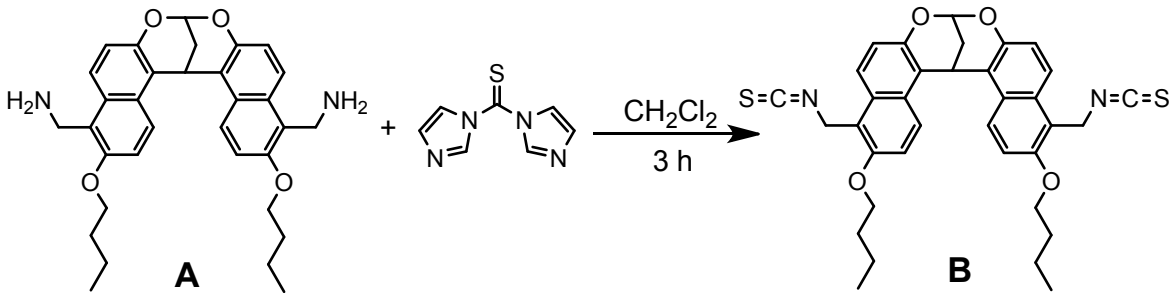

To the solution of 1, 1'-Thiocarbonyldiimidazole (524 mg, 3.0 mmol) in DCM (200 mL), were added compound **A** (527 mg, 1.0 mmol) and Hünig's base (258 mg, 2.0 mmol) were added dropwise during 30 min. The resulting mixture was stirred at room temperature for 3 h. The solvent was removed in vacuum, and the residue was purified by column chromatography (SiO_2, Hexane / DCM = 1 / 1) to give the compound **B** as a yellow solid (560 mg, 92 %). ^{1}H NMR (400 MHz, $CDCl_3$, 25 ^{o}C): δ [ppm] = 8.59 (d, J = 9.4 Hz, 2H), 7.72 (d, J = 9.2 Hz, 2H), 7.37 (d, J = 9.4 Hz, 2H), 7.30 (d, J = 9.2 Hz, 2H), 6.31 (s, 1H), 5.35 (s, 1H), 5.05 (dd, J = 13.0, 4.1 Hz, 2H),

1 Z. He, G. Ye and W. Jiang, *Chem. –Eur. J.* 2015, **21**, 3005-3012.

4.24-4.09 (m, 4H), 2.49 (s, 2H), 1.92-1.81 (m, 4H), 1.64-1.50 (m, 4H), 1.03 (t, J = 7.4 Hz, 6H). ^{13}C NMR (100 MHz, $CDCl_3$, 25 ^{o}C): δ [ppm] = 152.9, 148.8, 128.7, 126.5, 125.2, 122.6, 120.3, 119.0, 116.0, 114.2, 91.3, 69.3, 39.2, 31.5, 26.9, 23.0, 19.3, 13.9.

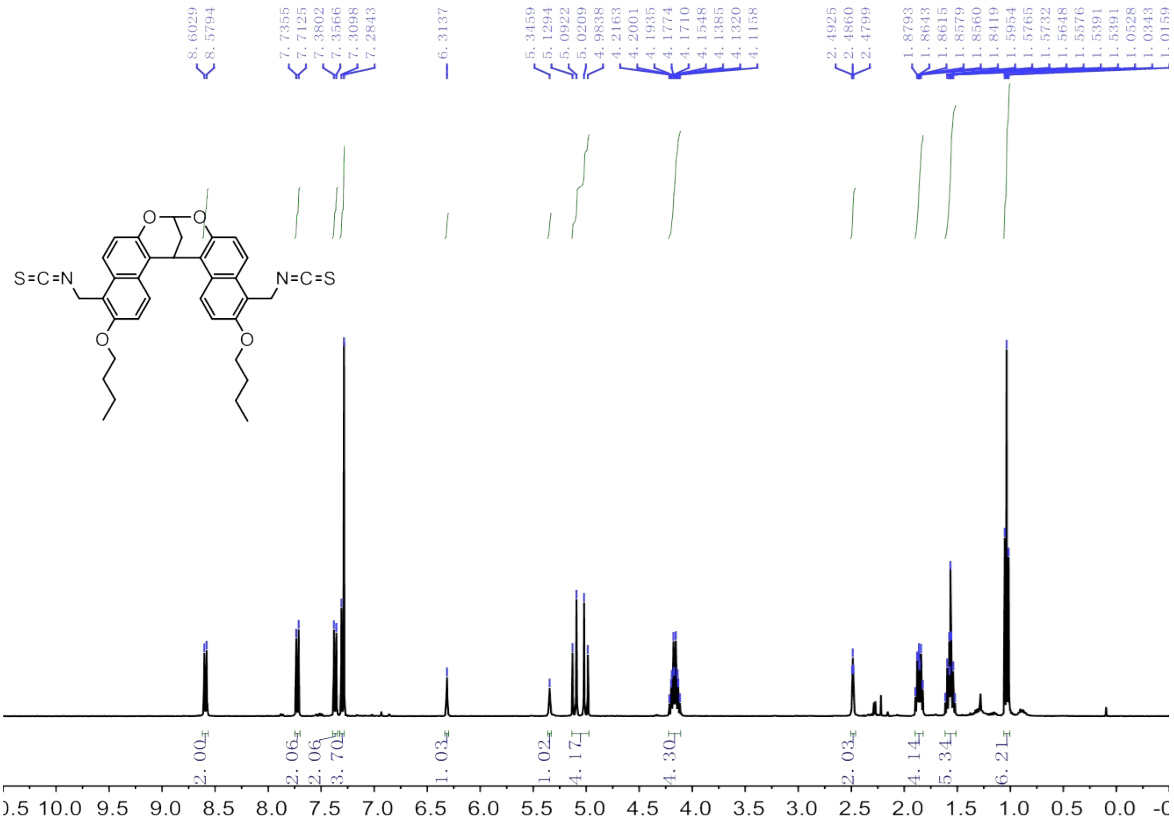

^{1}H NMR spectrum (400 MHz, $CDCl_3$, 25 ^{o}C) of compound **B**.

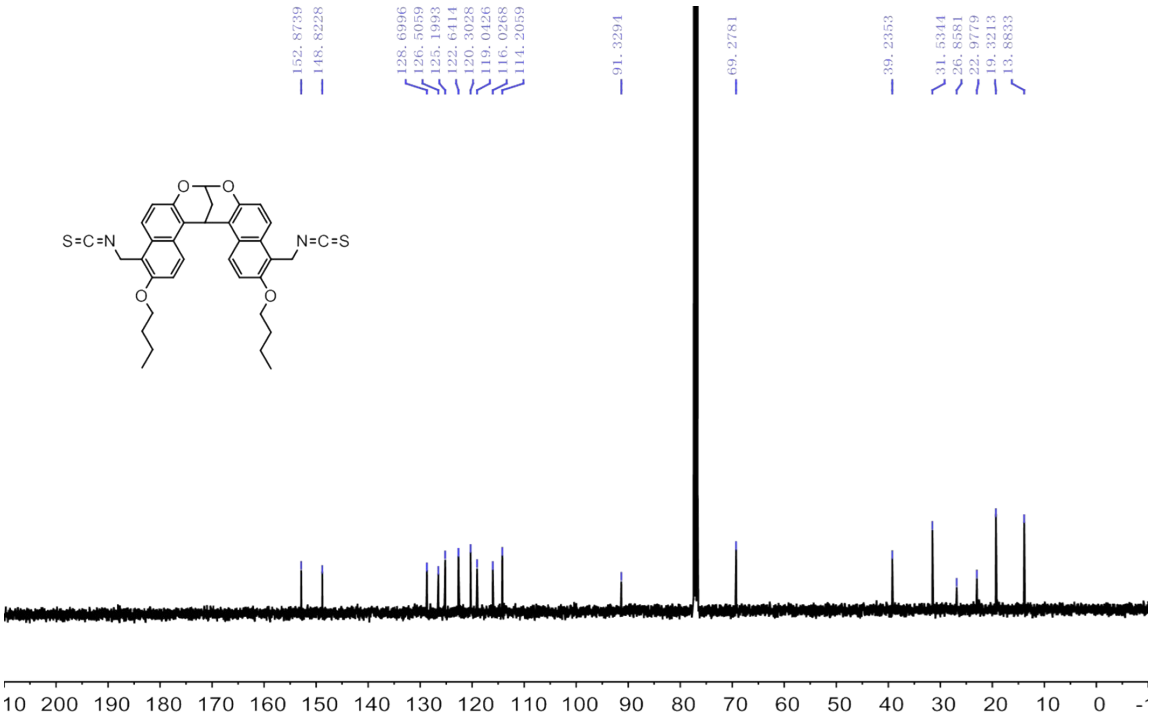

^{13}C NMR spectrum (100 MHz, $CDCl_3$, 25 ^{o}C) of compound **B**.

Compound 1b-anti/ 1b-syn

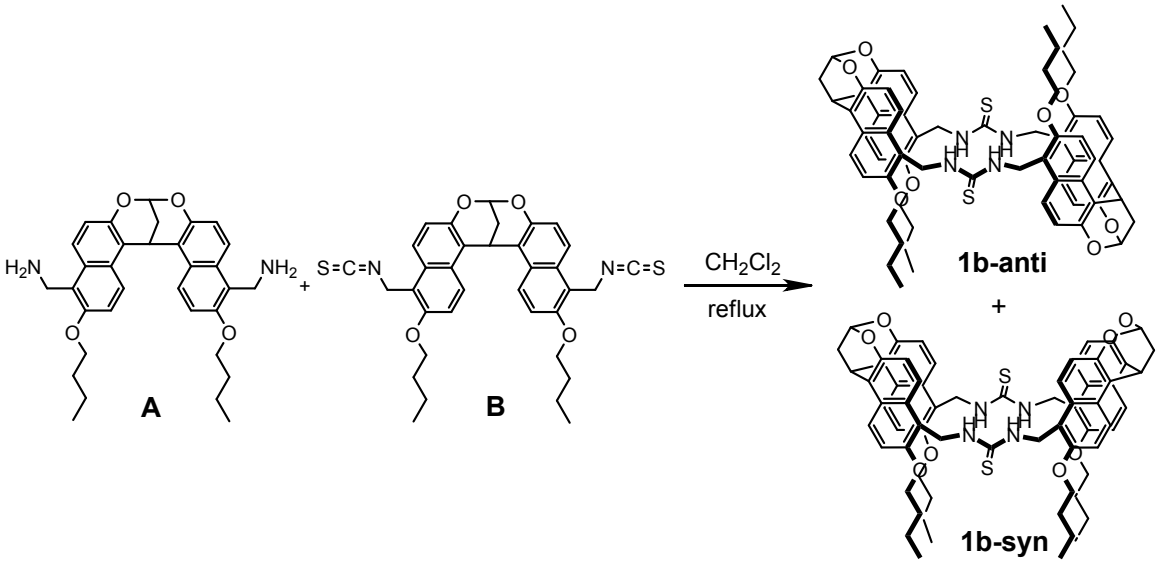

Compound 1b-anti/ 1b-syn

The solutions of compounds **A** (483 mg, 0.92 mmol; in 60 mL DCM) and **B** (560 mg, 0.92 mmol; in 60 mL DCM) in two separate syringes were added dropwise via a double-channel syring pump to the solution of Hünig's base (545 mg, 5.0 mmol) in DCM (400 mL) during the course of 10 h.

The resulting mixture was stirred overnight at reflux. After removing the solvent in vacuum, the residue was subjected to column chromatography (SiO_2, Hexane / DCM = 1 / 4) to afford the two isomers of macrocycle **1b**.

1b-anti. White solid, yield (84 mg, 8 %), m.p. > 320 °C (Decomposed); ^{1}H NMR (400 MHz, $CDCl_3$, 25 °C): δ [ppm] = 8.39 (d, *J* = 9.4 Hz, 2H), 7.53 (d, *J* = 9.2 Hz, 2H), 7.19 (d, *J* = 9.4 Hz, 2H), 7.06 (d, *J* = 9.2 Hz, 2H), 6.22 (s, 1H), 5.25 (s, 1H), 5.23 (dd, *J* = 13.2, 4.1 Hz, 2H), 4.86 (dd, *J* = 13.2, 4.1 Hz, 2H), 4.61 (t, *J* = 9.4 Hz, 2H), 4.06-3.95 (m, 4H), 2.45 (s, 2H), 1.82-1.75 (m, 4H), 1.52-1.47 (m, 4H), 1.00 (t, *J* = 7.4 Hz, 6H). ^{13}C NMR (100 MHz, $CDCl_3$, 25 °C): δ [ppm] = 181.8, 153.0, 148.6, 128.9, 126.3, 124.5, 123.1, 119.6, 119.2, 118.8, 114.4, 91.3, 69.4, 39.3, 31.6, 26.5, 22.7, 19.3, 14.0. ESI-TOF-HRMS: *m/z* calcd for $[M+H]^+$ $C_{68}H_{73}N_4O_8S_2^+$, 1137.4864; found 1137.4873 (error = +0.8 ppm).

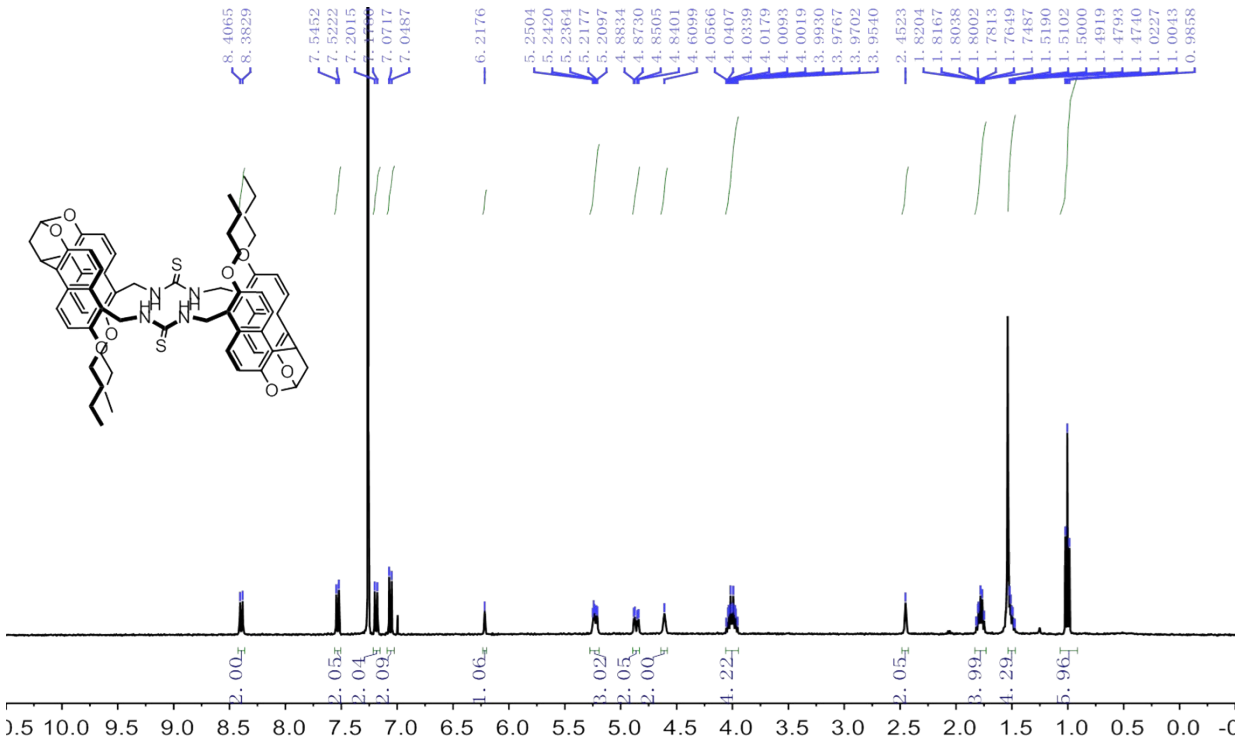

^{1}H NMR spectrum (400 MHz, $CDCl_3$, 25 °C) of compound **1b-anti**.

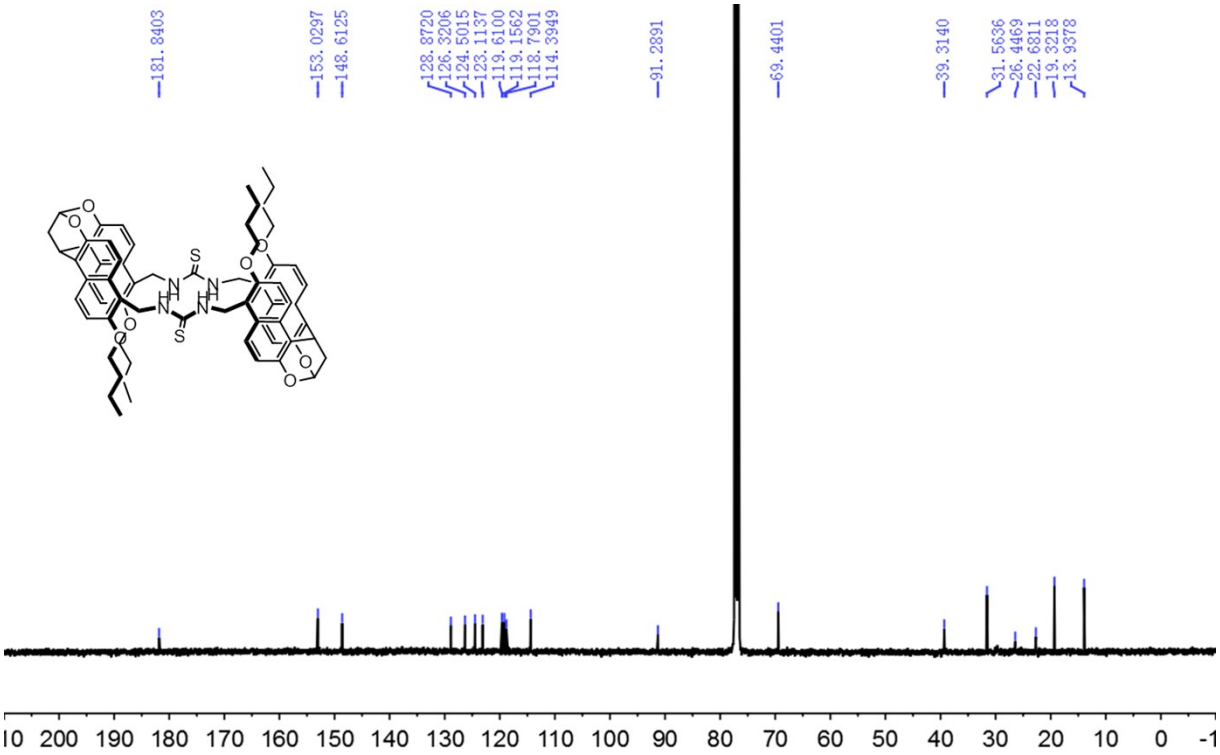

^{13}C NMR spectrum (100 MHz, $CDCl_3$, 25 ^{o}C) of compound **1b-anti**.

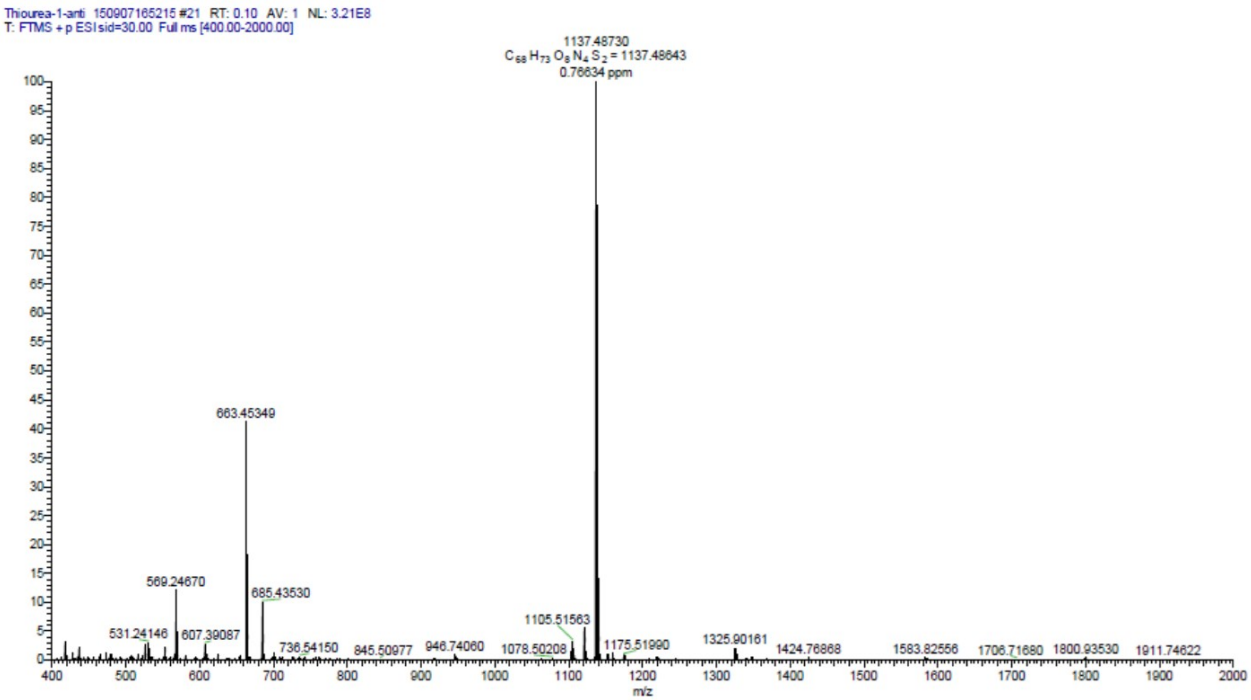

ESI mass spectrum of compound **1b-anti**.

1b-syn. White solid, yield (220 mg, 21 %), m.p. > 320 °C (Decomposed); ^{1}H NMR (400 MHz, $CDCl_3$, 25 °C): δ [ppm] = 8.37 (d, *J* = 9.4 Hz, 2H), 7.67 (d, *J* = 9.2 Hz, 2H), 7.15 (dd, *J* = 9.4, 9.2 Hz, 4H), 6.26 (s, 1H), 5.40 (dd, *J* = 13.2, 6.9 Hz, 2H), 5.21 (s, 1H), 4.85 (d, *J* = 13.2 Hz, 2H), 4.71 (d, *J* = 6.9 Hz, 2H), 4.05-3.95 (m, 4H), 2.45 (s, 2H), 1.77-1.70 (m, 4H), 1.49-1.44 (m, 4H), 0.96 (t, *J* = 7.4 Hz, 6H). ^{13}C NMR (100 MHz, $CDCl_3$, 25 °C): δ [ppm] = 181.3, 152.9, 148.9, 129.0, 126.5, 124.4, 123.8, 120.0, 119.1, 118.9, 114.0, 91.2, 69.4, 39.3, 31.6, 26.5, 22.8, 19.3, 13.9. ESI-TOF-HRMS: *m/z* calcd for $[M+H]^+$ $C_{68}H_{73}N_4O_8S_2^+$, 1137.4864; found 1137.4844 (error = -1.8 ppm).

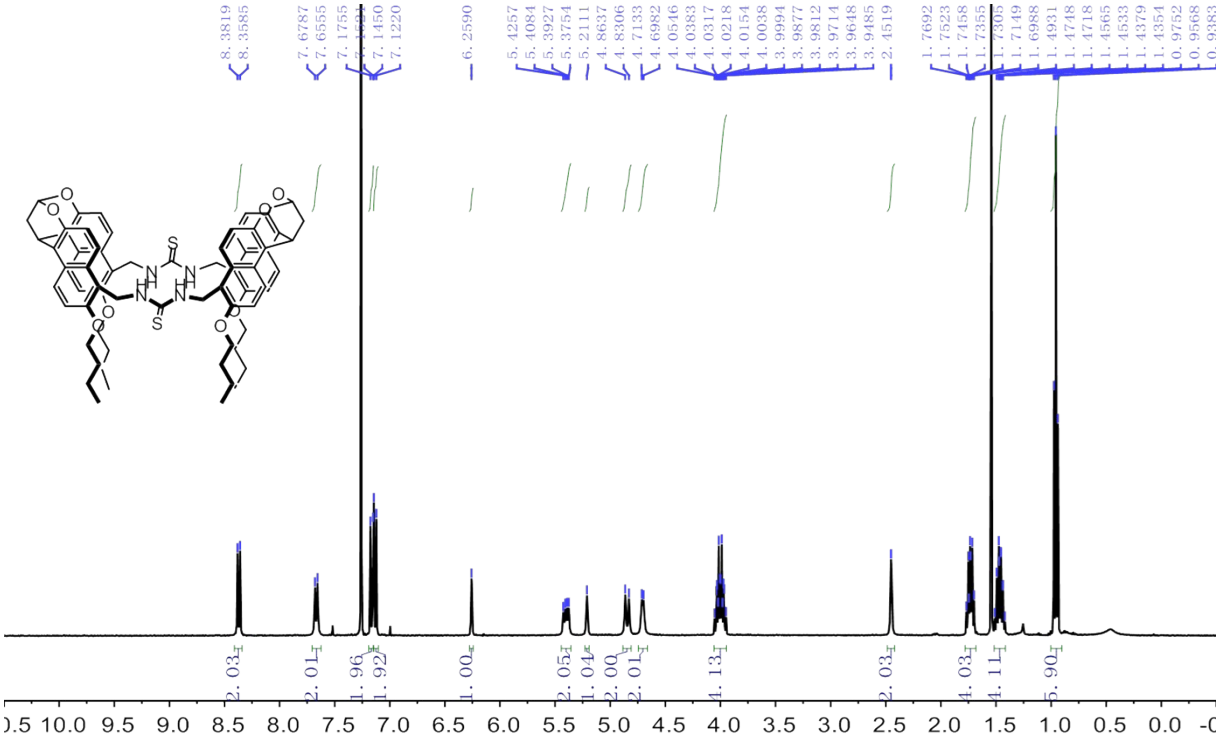

^{1}H NMR spectrum (400 MHz, $CDCl_3$, 25 °C) of compound **1b-syn**.

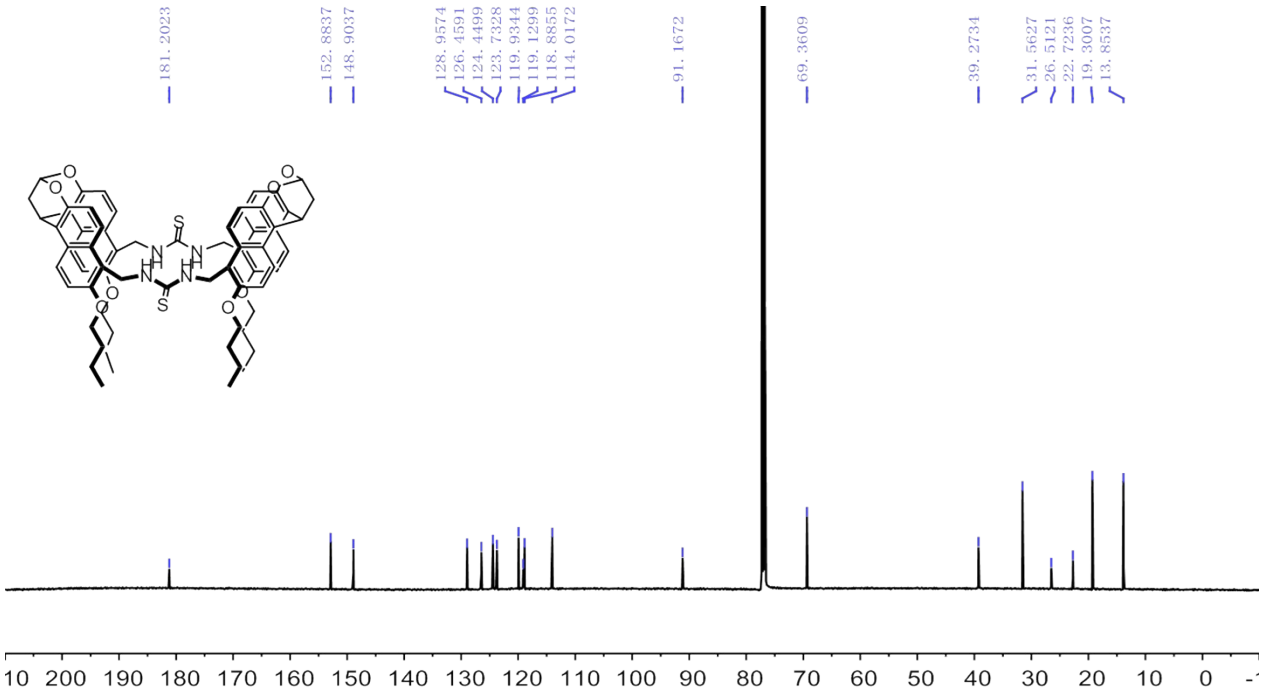

^{13}C NMR spectrum (100 MHz, $CDCl_3$, 25 ^{o}C) of compound **1b-syn**.

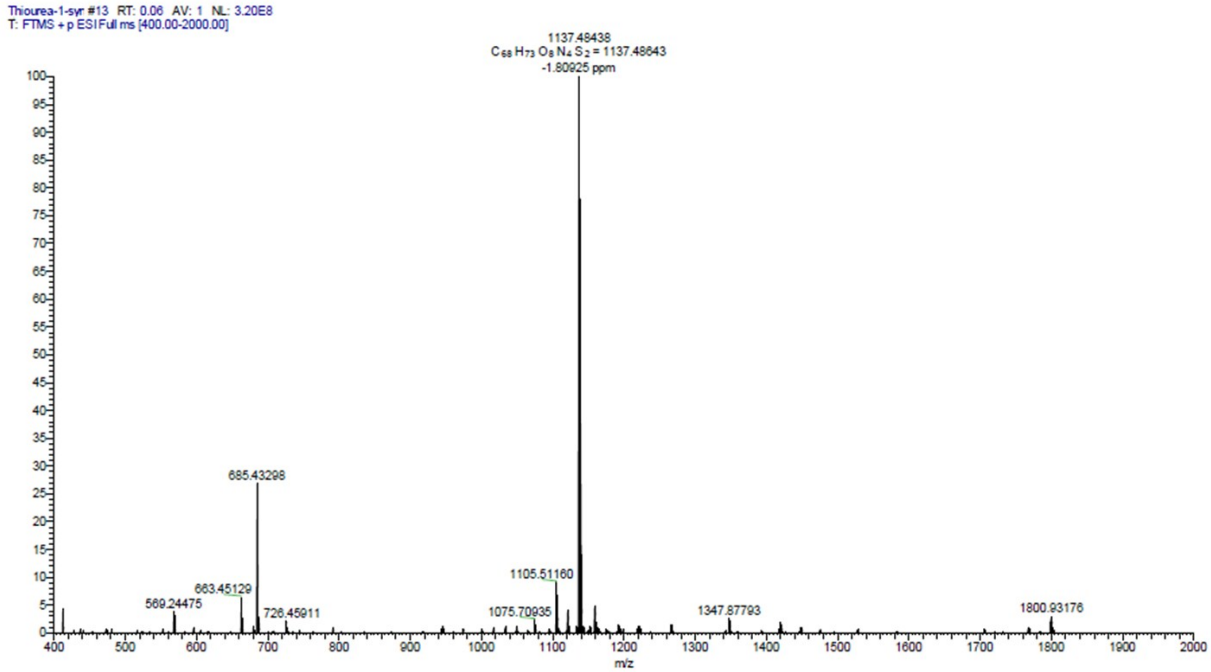

ESI-TOF mass spectrum of compound **1b-syn**.

3. Single Crystal Structure

Single crystal X-ray data for **1b-anti** was collected at 120.0(1) K with Agilent Super-Nova dual wavelength diffractometer with a micro-focus X-ray source and multilayer optics monochromatized Cu-*K*α (λ = 1.54184 Å) radiation. Program *CrysAlisPro*[2] was used for the data collection and reduction. The intensities were corrected for absorption using analytical face index absorption correction method[3] for all the data. The structures were solved with direct methods (*SHELXS*[4]) and refined by full-matrix least squares on F^2 using the *OLEX2*[54], which utilizes the *SHELXL*-2014 module[3]. Anisotropic displacement parameters were assigned to non-H atoms. All hydrogen atoms (except N-*H*) were refined using riding models with U_{eq}(H) of 1.5U_{eq}(C) for terminal methyl groups, and 1.2 U_{eq}(C) for other groups. The hydrogens bonded to N atoms were found from the difference Fourier maps and refined with the ideal N-H distances (0.91 Å) and U_{eq}(H) of 1.2 U_{eq}(N). Two chloride atoms of one cocrystallized $CHCl_3$ show disorder over two positions according to the difference Fourier maps. Anisotropic displacement parameters and geometry of the disordered molecule were restrained. The details of the crystals data, data collection, and the refinement results are documented below.

Crystal data: **1b-anti**: 0.22×0.12×0.04 mm, $C_{75}H_{81}N_6O_8S_2Cl_9$, M = 1577.62, triclinic, space group P-1, a = 12.1788(4) Å, b = 13.6793(5) Å, c = 24.8910(6) Å, α = 89.173(2)°, β = 85.674(2)°, γ = 65.484(3)°, V = 3761.5(2) Å^3, Z = 2, ρ = 1.39 g cm^{-3}, μ = 4.06 mm^{-1}, F(000) = 1644, 58494 reflections (θ_{max} = 67.49°) measured (13112 unique, R_{int} = 0.037, completeness = 96.3%), Final R indices ($I > 2\sigma(I)$): R_1= 0.040, wR_2 = 0.100, R indices (all data): R_1= 0.050, wR_2 = 0.107. GOF = 1.02 for 932 parameters and 48 restraints, largest diff. peak and hole 0.61/–0.66 eÅ^{-3}. CCDC-1443004 contains the supplementary data for this structure. These data can be obtained free of charge via www.ccdc.cam.ac.uk/data_request/cif, or by emailing data_request@ccdc.cam.ac.uk, or by contacting The Cambridge Crystallographic Data Centre, 12, Union Road, Cambridge CB2 1EZ, UK; fax: +44 1223 336033

---

2 *CrysAlisPro* 2012, Agilent Technologies. Version 1.171.36.31.
3 Clark, R. C.; Reid, J. S. *Acta Cryst.* 1995, **A51**, 887.
4 Sheldrick, G. M. *Acta Crystallogr.* 2008, **A64**, 112–122.
5 Dolomanov, O. V.; Bourhis, L. J.; Gildea, R. J.; Howard, J. A. K. and Puschmann H., *J. Appl. Cryst.* 2009, **42**, 339-341.

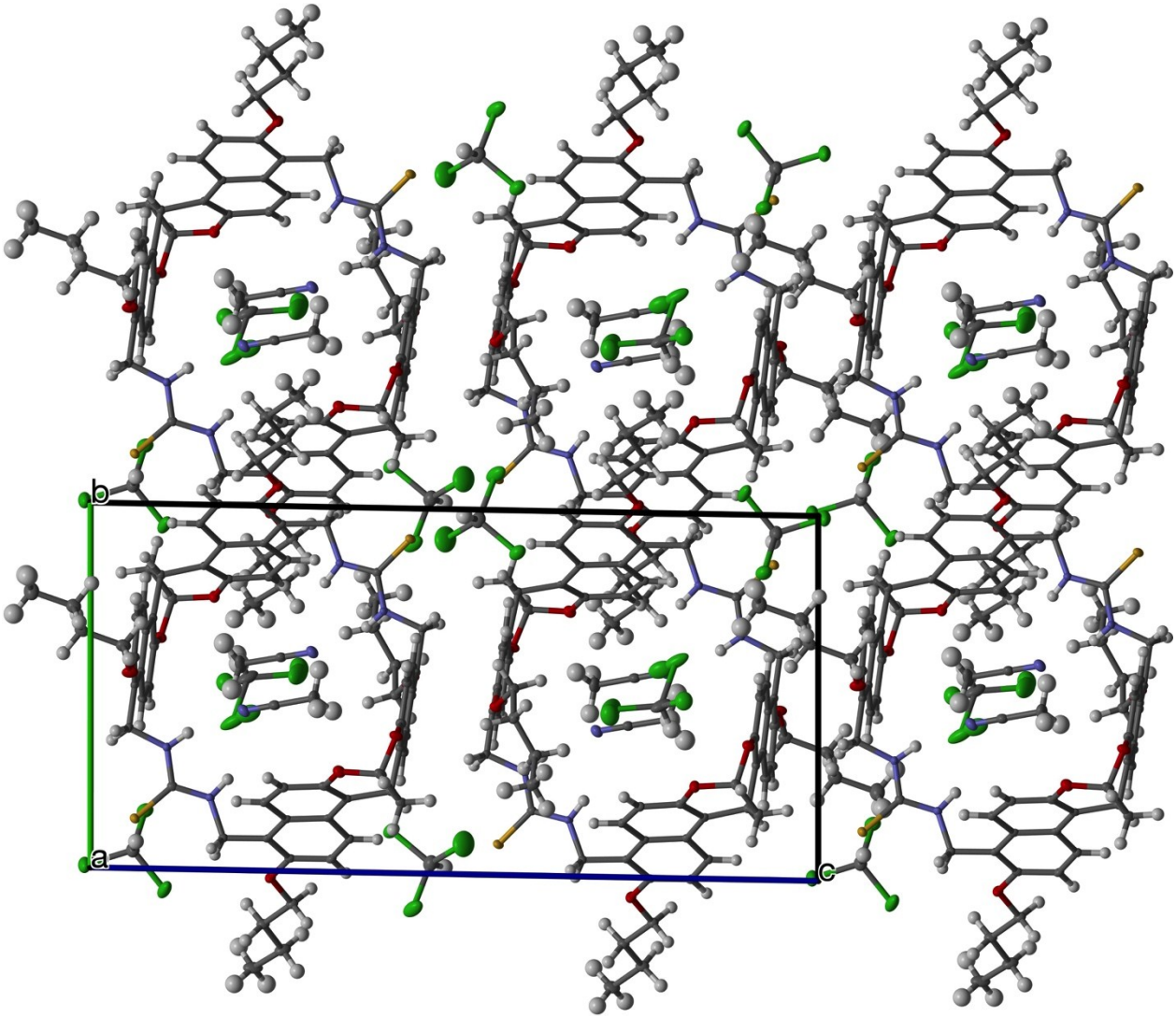

Fig. S1 The crystal packing of **1b-anti** along the crystallographic *a*-axis. The thermal ellipsoids of all non-H atoms are drawn at 30% probability level.

4. NMR Spectra of Host-Guest Complexes.

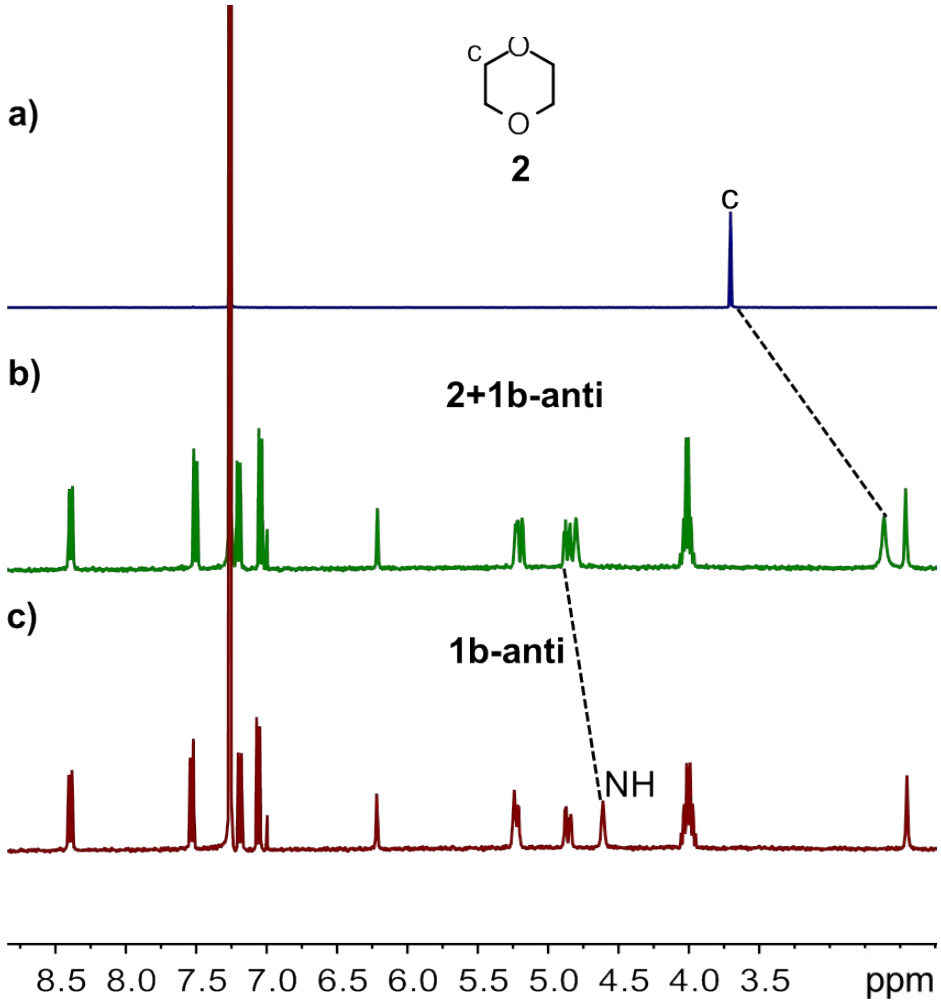

Fig. S2 ^{1}H NMR spectra (400 MHz, $CDCl_3$, 25 ^{o}C) of (a) guest **2**, (c) **1b-anti**, and (b) its equimolar mixture. The proton *c* of the guest experiences the upfield shift, the proton NH of the host experiences the downfield shift, suggesting that the complexation between **1b-anti** and guest **2**.

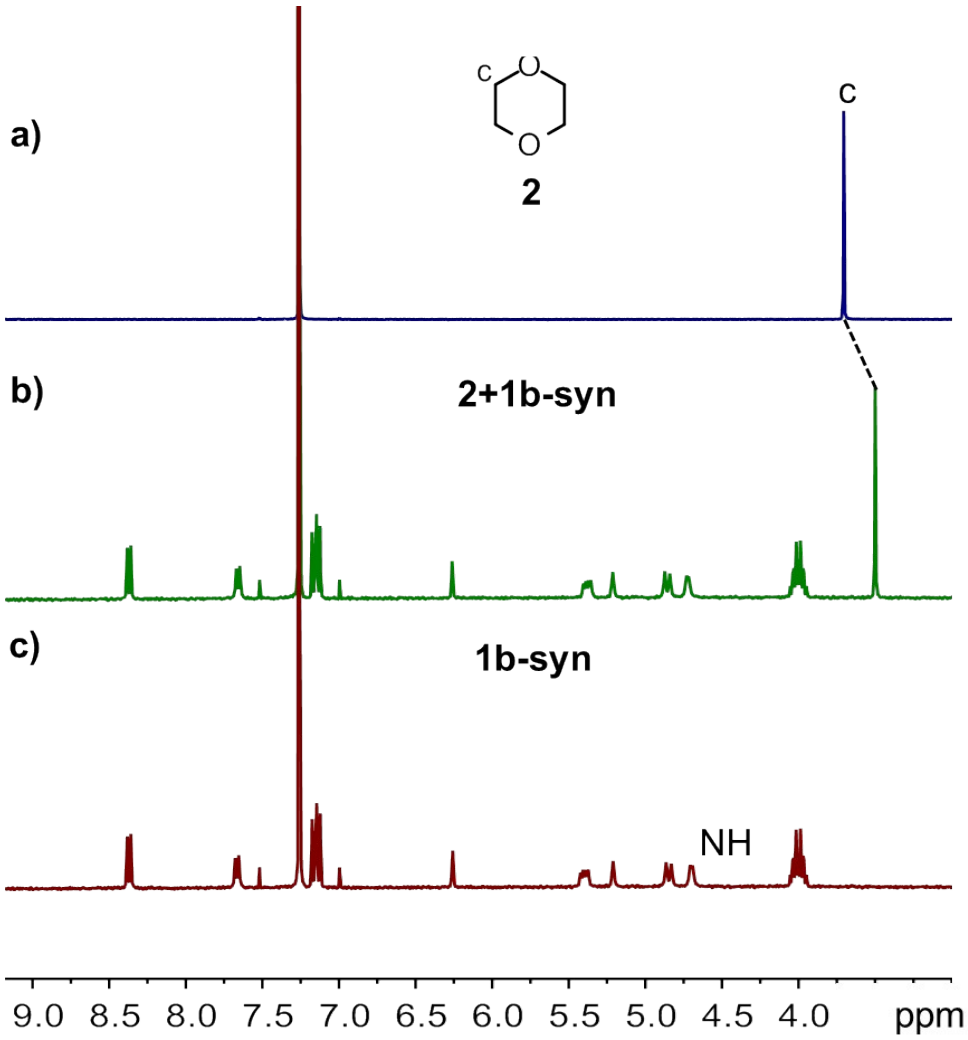

Fig. S3 ^{1}H NMR spectra (400 MHz, $CDCl_3$, 25 ^{o}C) of (a) guest **2**, (c) **1b-syn**, and (b) its equimolar mixture. The proton *c* of the guest experiences the upfield shift, suggesting that the complexation between **1b-syn** and guest **2**.

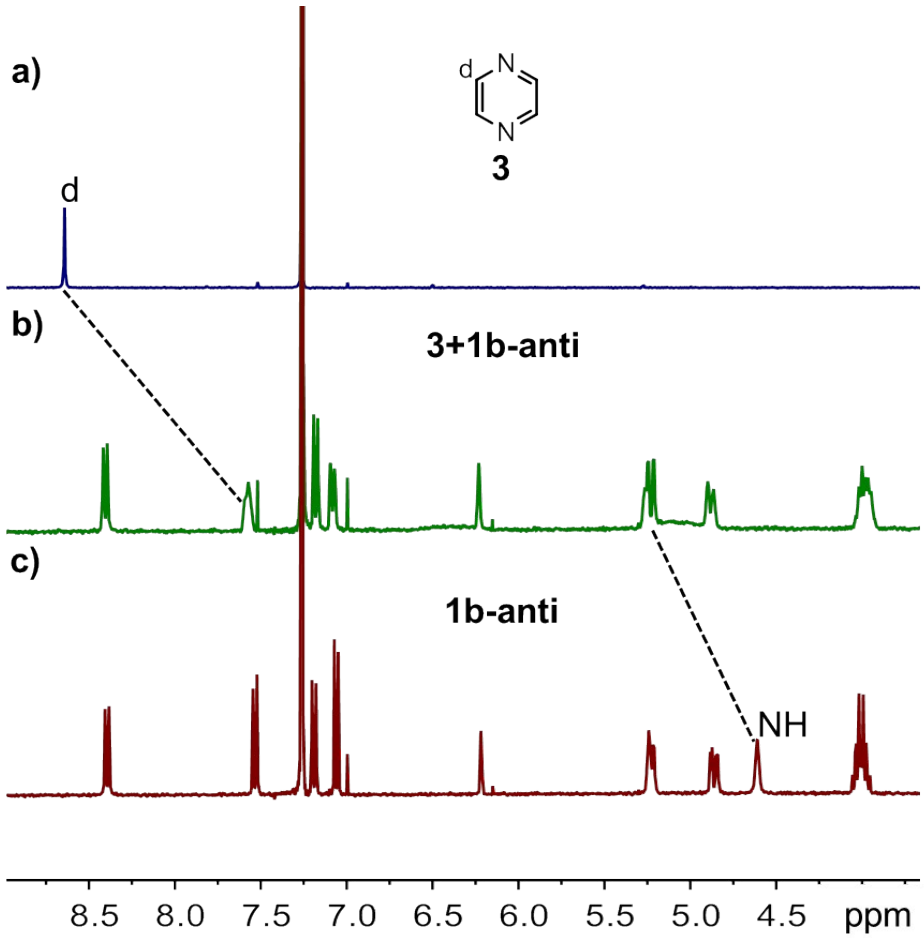

Fig. S4 ^{1}H NMR spectra (400 MHz, $CDCl_3$, 25 ^{o}C) of (a) guest **3**, (c) **1b-anti**, and (b) its equimolar mixture. The proton *d* of the guest experiences the upfield shift, the proton NH of the host experiences the downfield shift, suggesting that the complexation between **1b-anti** and guest **3**.

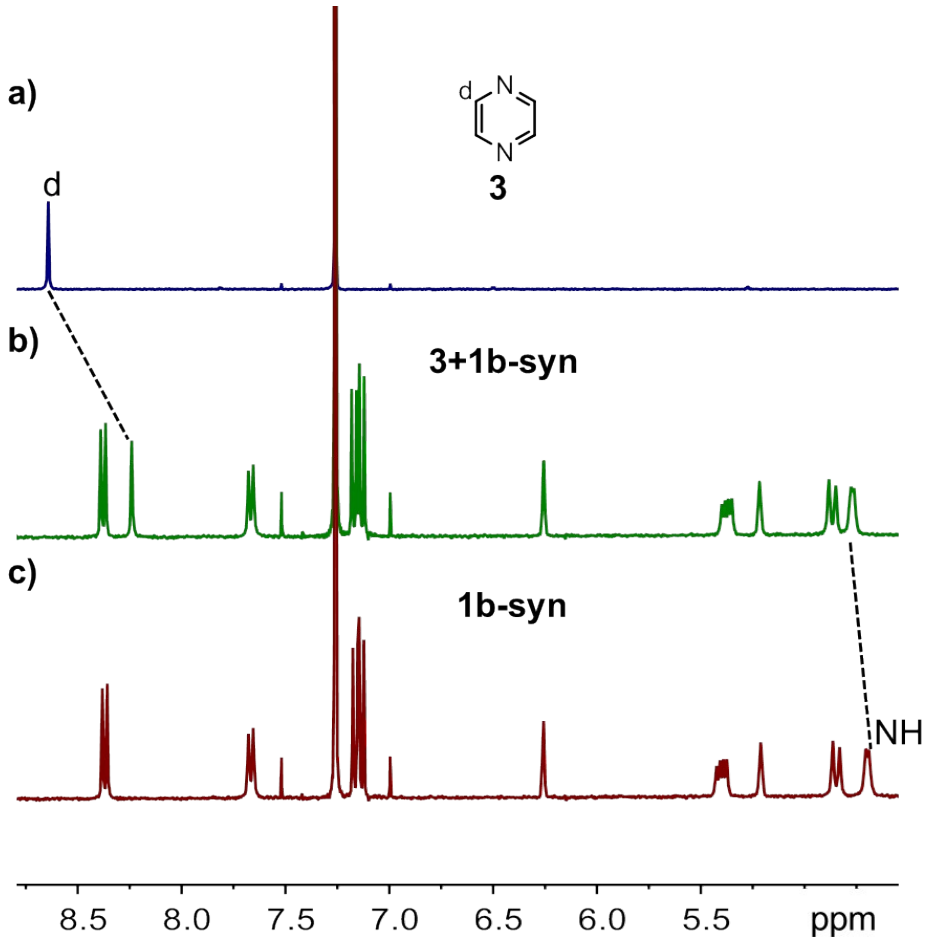

Fig. S5 ^{1}H NMR spectra (400 MHz, $CDCl_3$, 25 ^oC) of (a) guest **3**, (c) **1b-syn**, and (b) its equimolar mixture. The proton *d* of the guest experiences the large upfield shift, the proton NH of the host experiences the downfield shift, suggesting that the complexation between **1b-syn** and guest **3**.

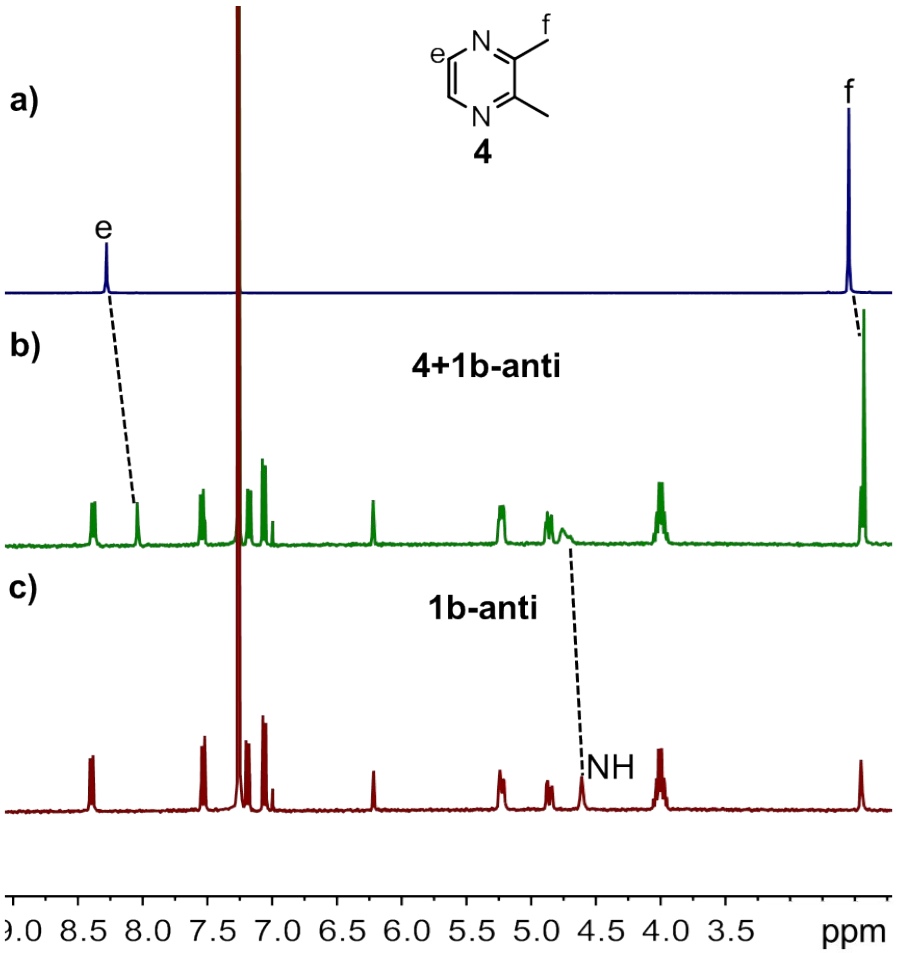

Fig. S6 ^{1}H NMR spectra (400 MHz, $CDCl_3$, 25 ^{o}C) of (a) guest **4**, (c) **1b-anti**, and (b) its equimolar mixture. The proton *e* and *f* of the guest experiences the upfield shift, the proton NH of the host experiences the downfield shift, suggesting that the complexation between **1b-anti** and guest **4**.

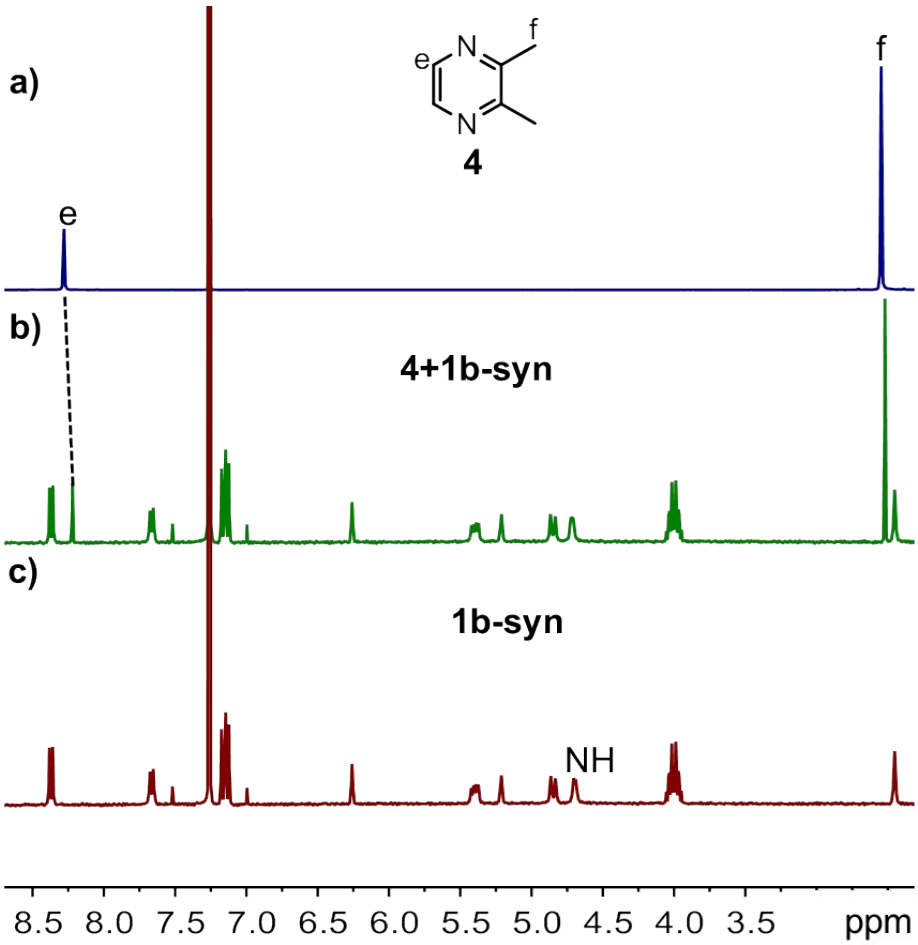

Fig. S7 ^{1}H NMR spectra (400 MHz, $CDCl_3$, 25 ^{o}C) of (a) guest **4**, (c) **1b-syn**, and (b) its equimolar mixture. The proton *e* and *f* of the guest experiences the large upfield shift, suggesting that the complexation between **1b-syn** and guest **4**.

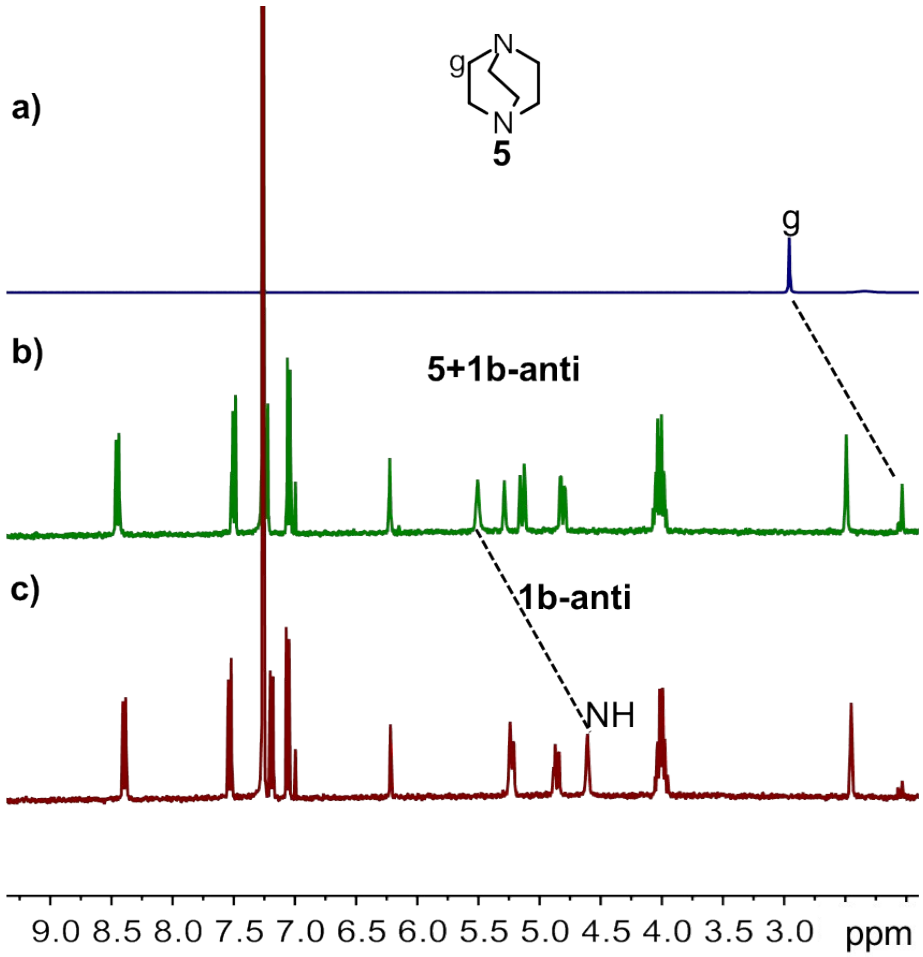

Fig. S8 ^{1}H NMR spectra (400 MHz, $CDCl_3$, 25 ^{o}C) of (a) guest **5**, (c) **1b-anti**, and (b) its equimolar mixture. The proton *g* of the guest experiences the upfield shift, the proton NH of the host experiences the downfield shift, suggesting that the complexation between **1b-anti** and guest **5**.

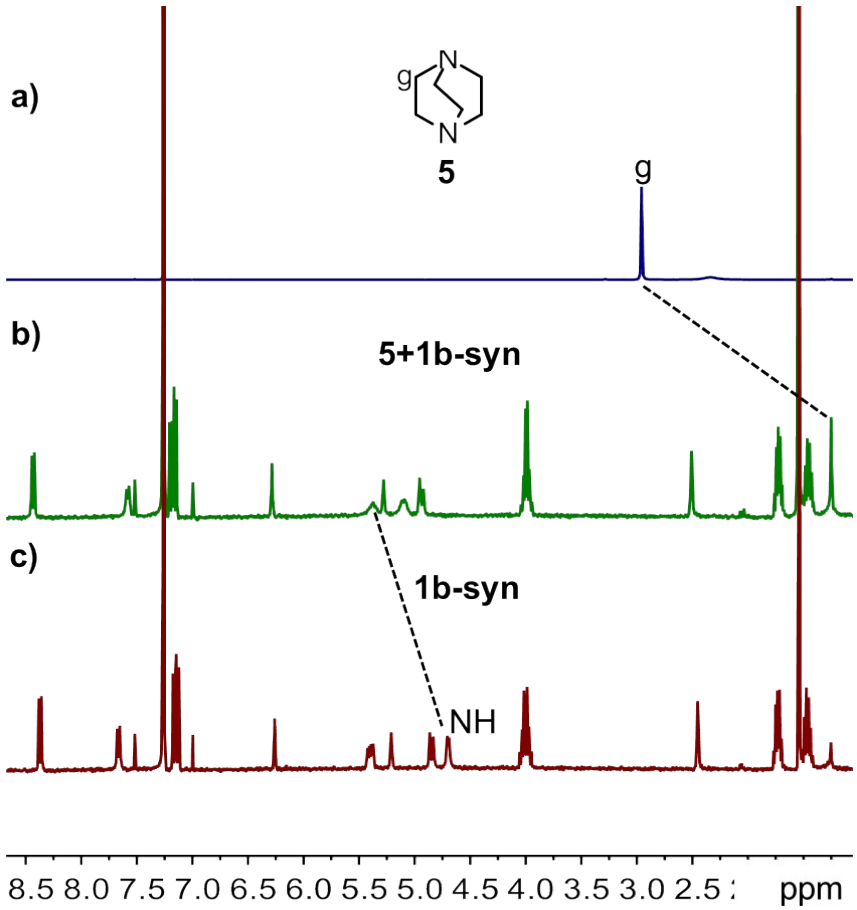

Fig. S9 ^{1}H NMR spectra (400 MHz, $CDCl_3$, 25 ^{o}C) of (a) guest **5**, (c) **1b-syn**, and (b) its equimolar mixture. The proton *g* of the guest experiences the large upfield shift, the proton NH of the host experiences the downfield shift, suggesting that the complexation between **1b-syn** and guest **5**.

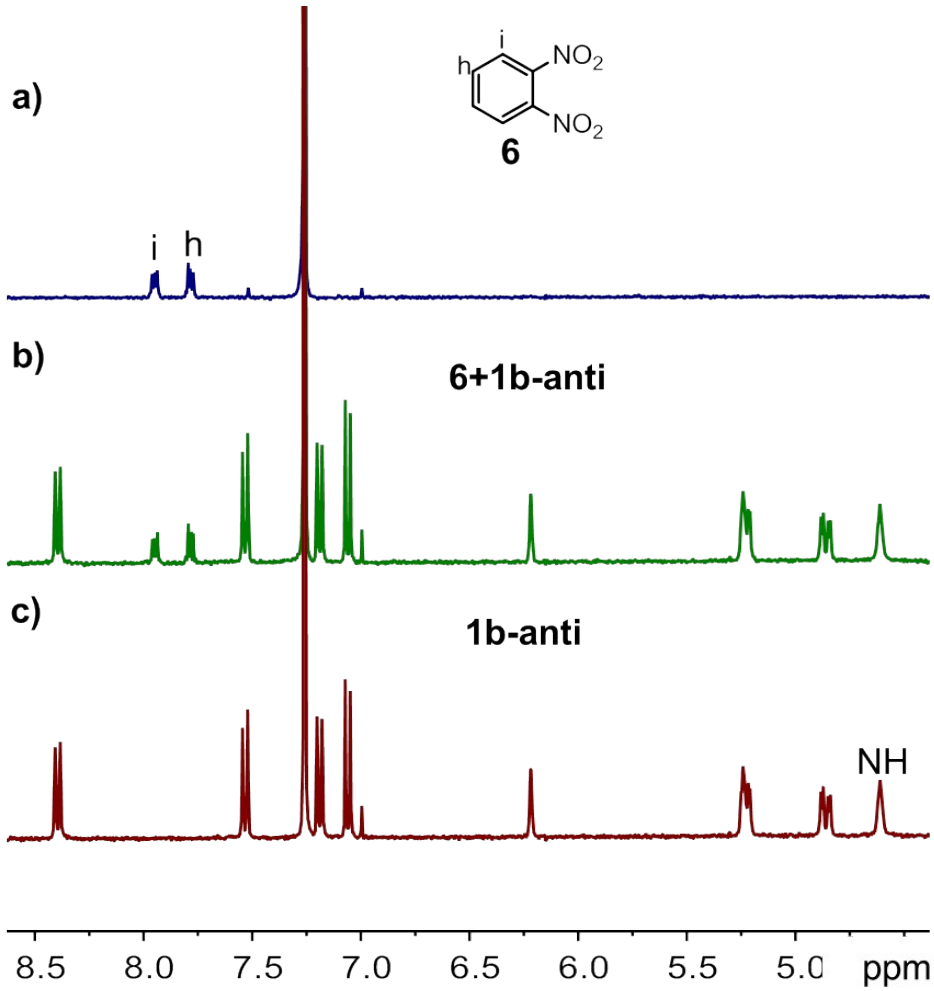

Fig. S10 ^{1}H NMR spectra (400 MHz, $CDCl_3$, 25 ^{o}C) of (a) guest **6**, (c) **1b-anti**, and (b) its equimolar mixture. The protons *h* and *i* of the guest undergo no shift at all, suggesting no complexation between **1b-anti** and guest **6**.

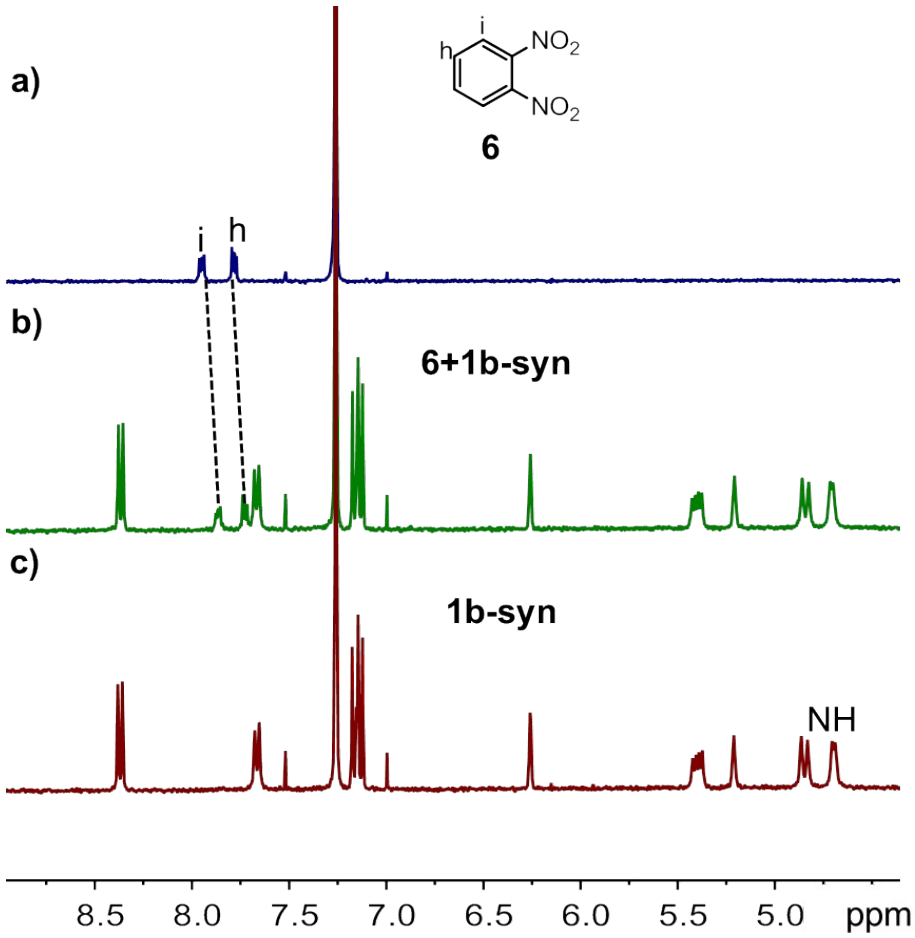

Fig. S11 ^{1}H NMR spectra (400 MHz, $CDCl_3$, 25 ^{o}C) of (a) guest **6**, (c) **1b-syn**, and (b) its equimolar mixture. The protons *h* and *i* of the guest experiences upfield shift, suggesting that the complexation between **1b-syn** and guest **6**.

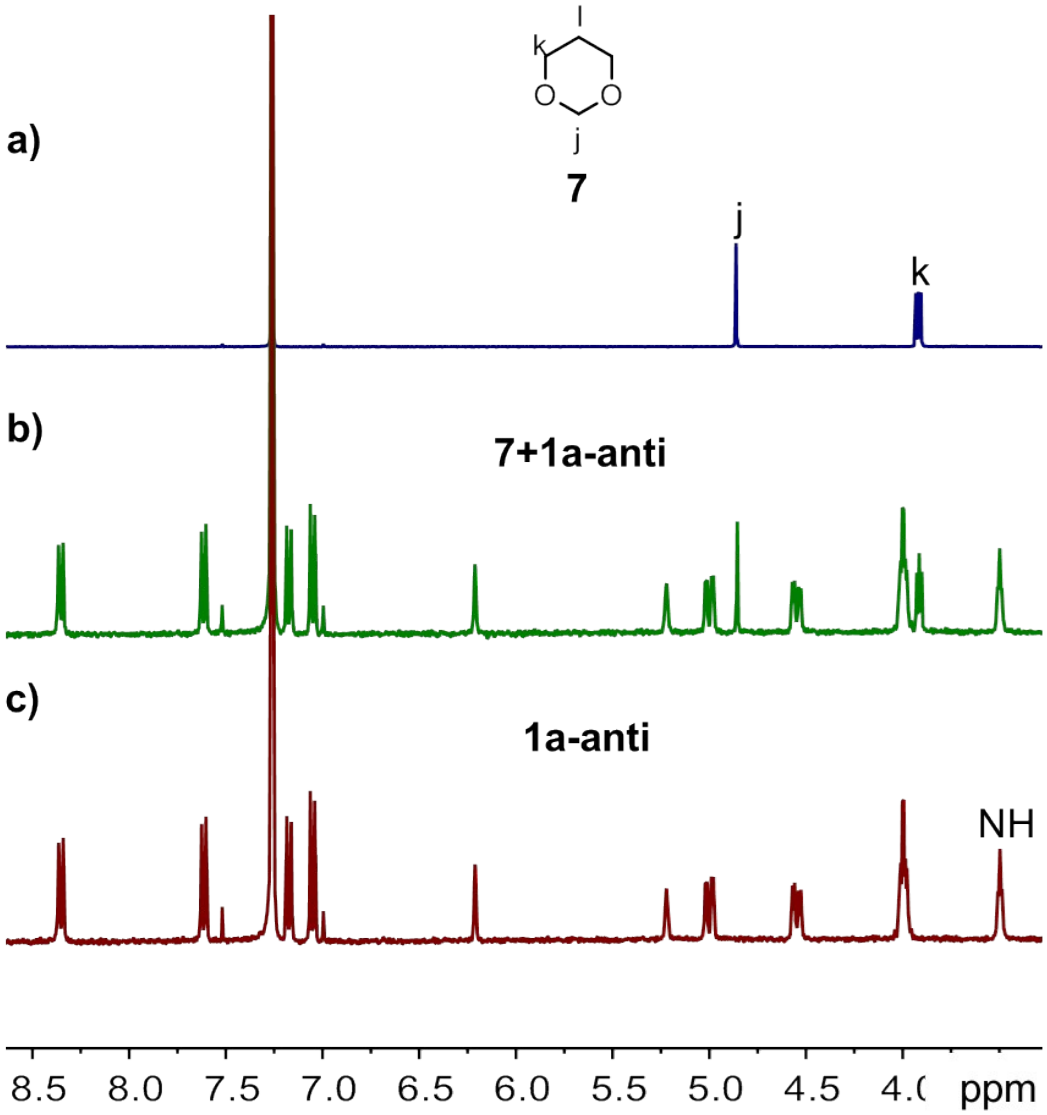

Fig. S12 ^{1}H NMR spectra (400 MHz, $CDCl_3$, 25 ^{o}C) of (a) guest **7**, (c) **1a-anti**, and (b) its equimolar mixture. No obvious change on NH protons was observed, the protons *j* and *k* of the guest undergo no shift at all, suggesting very weak binding between **1a-anti** and guest **7**.

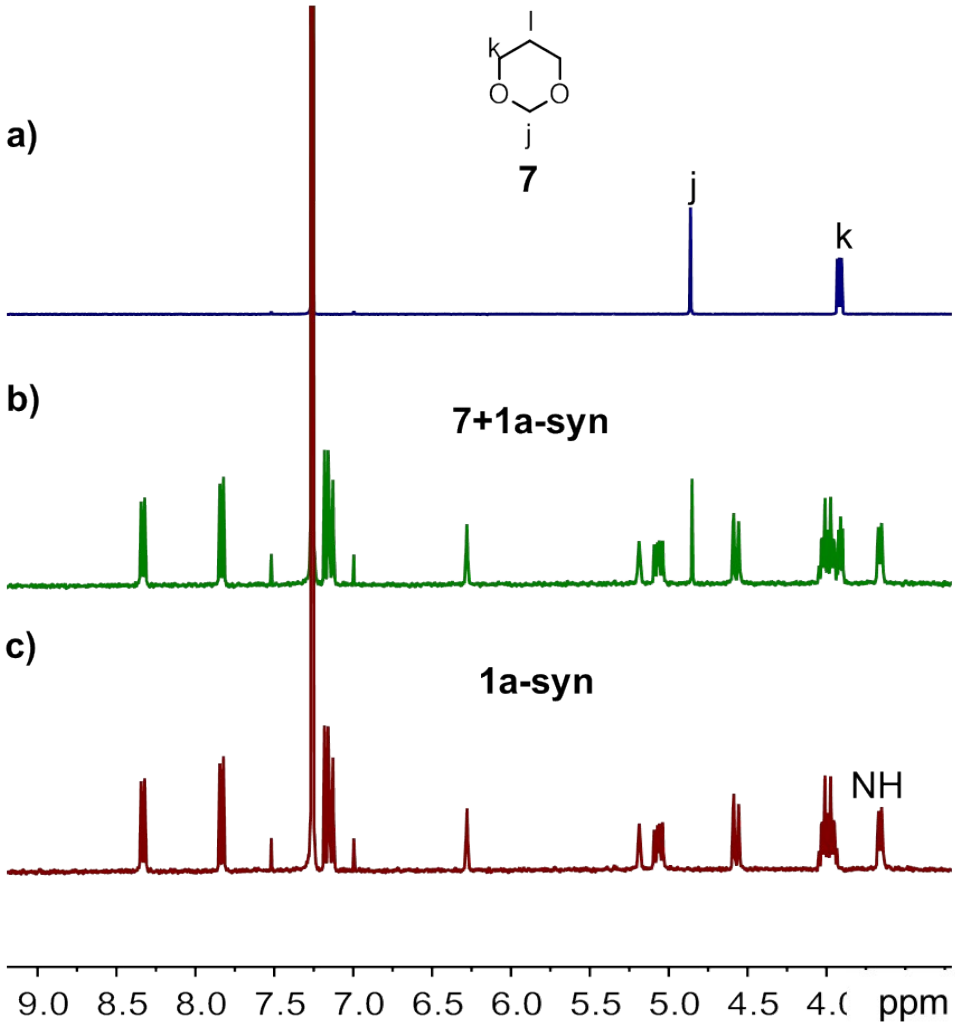

Fig. S13 ^{1}H NMR spectra (400 MHz, $CDCl_3$, 25 ^{o}C) of (a) guest **7**, (c) **1a-syn**, and (b) its equimolar mixture. No obvious change on NH protons was observed, the protons *j* and *k* of the guest undergo no shift at all, suggesting very weak binding between **1a-syn** and guest **7**.

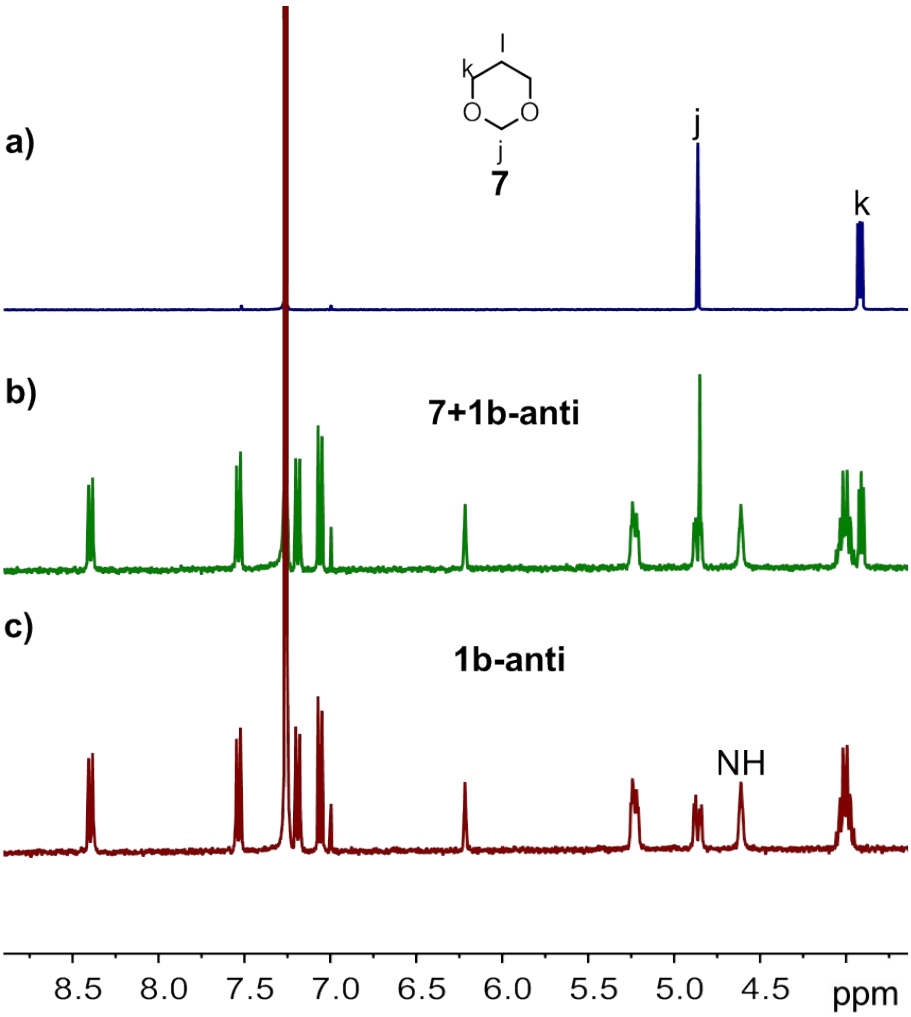

Fig. S14 ^{1}H NMR spectra (400 MHz, $CDCl_3$, 25 ^oC) of (a) guest **7**, (c) **1b-anti**, and (b) its equimolar mixture. No obvious change on NH protons was observed, the protons *j* and *k* of the guest undergo no shift at all, suggesting very weak binding between **1b-anti** and guest **7**.

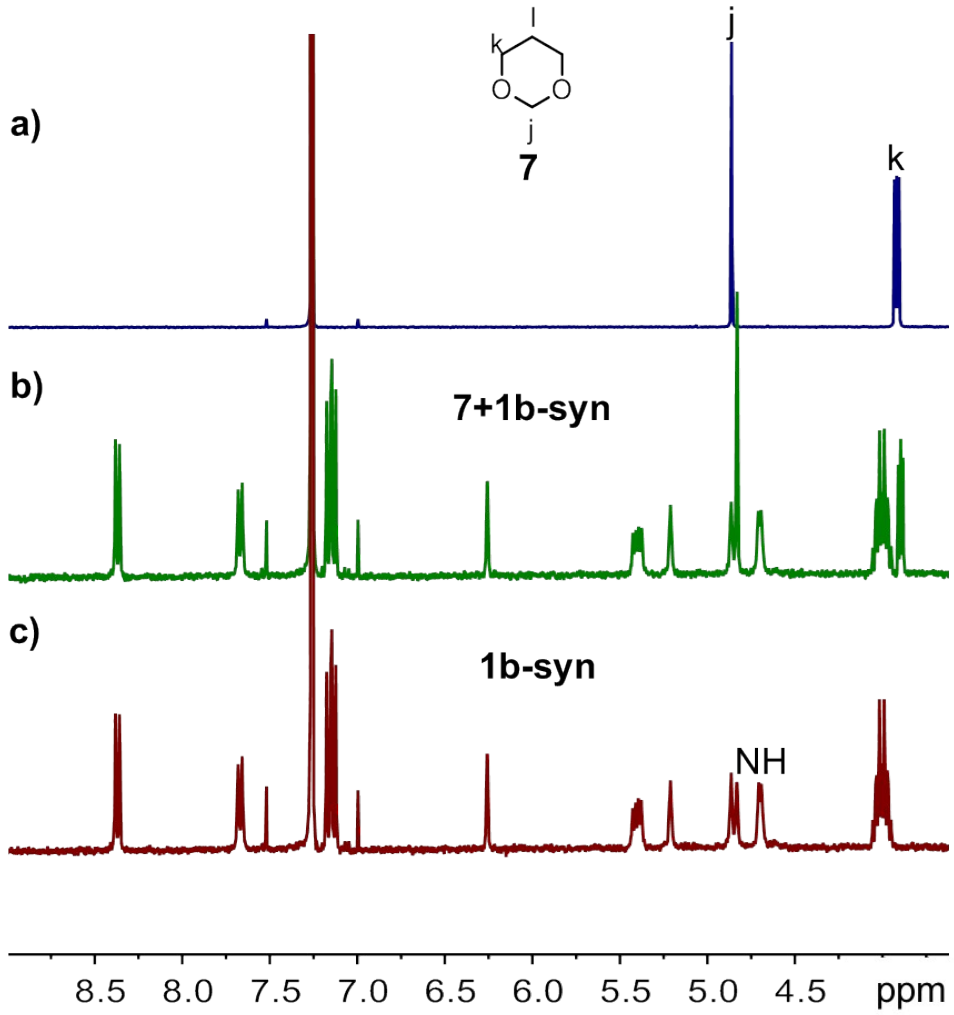

Fig. S15 ^{1}H NMR spectra (400 MHz, $CDCl_3$, 25 ^oC) of (a) guest **7**, (c) **1b-syn**, and (b) its equimolar mixture. No obvious change on NH protons was observed, the protons *j* and *k* of the guest undergo no shift at all, suggesting very weak binding between **1b-syn** and guest **7**.

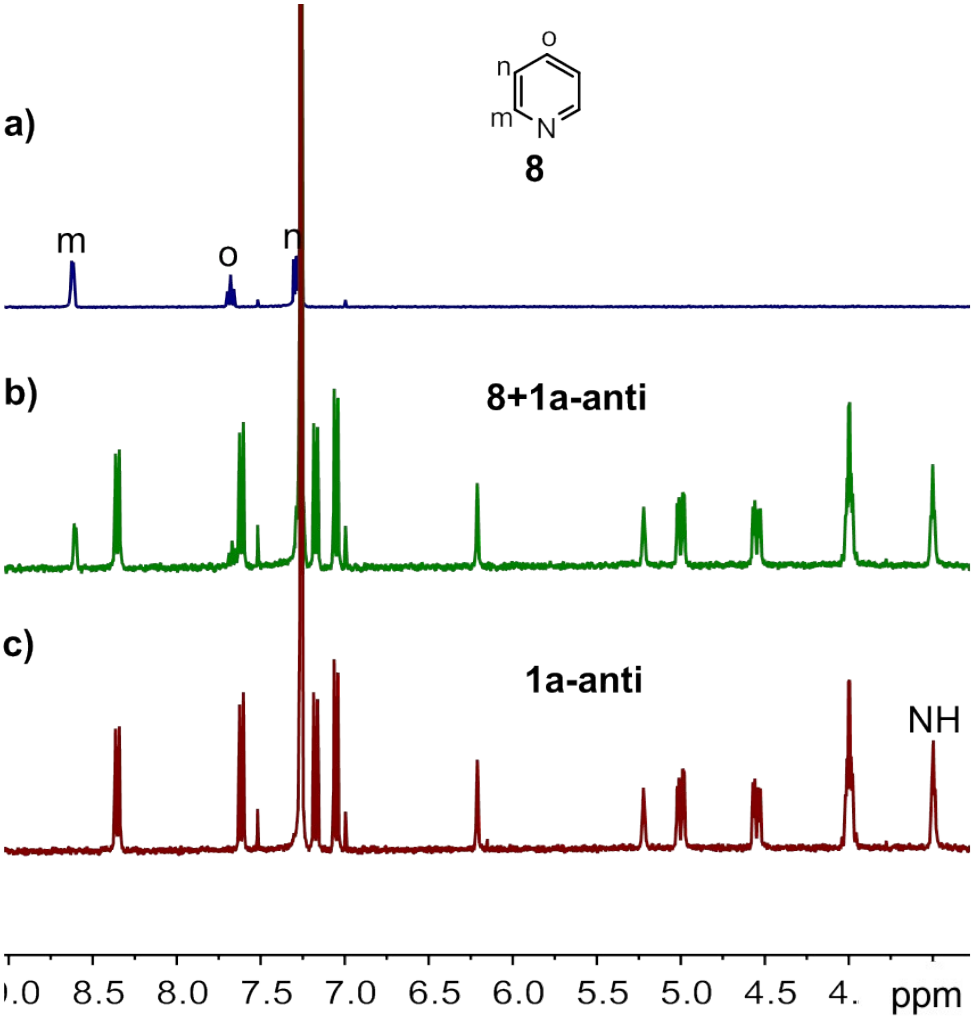

Fig. S16 ^{1}H NMR spectra (400 MHz, $CDCl_3$, 25 ^{o}C) of (a) guest **8**, (c) **1a-anti**, and (b) its equimolar mixture. No obvious change on NH protons was observed, the protons *m, n* and *o* of the guest undergo no shift at all, suggesting very weak binding between **1a-anti** and guest **8**.

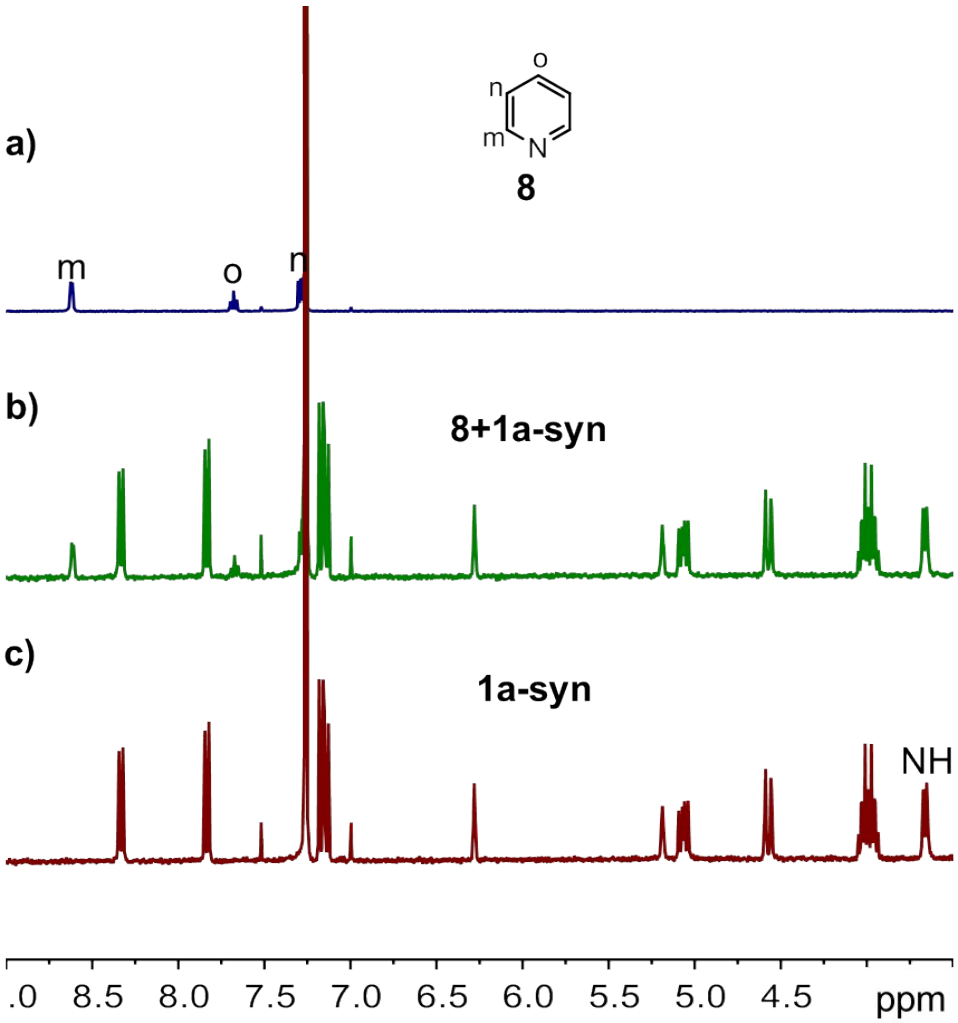

Fig. S17 ^{1}H NMR spectra (400 MHz, $CDCl_3$, 25 ^{o}C) of (a) guest **8**, (c) **1a-syn**, and (b) its equimolar mixture. No obvious change on NH protons was observed, the protons *m, n* and *o* of the guest undergo no shift at all, suggesting very weak binding between **1a-syn** and guest **8**.

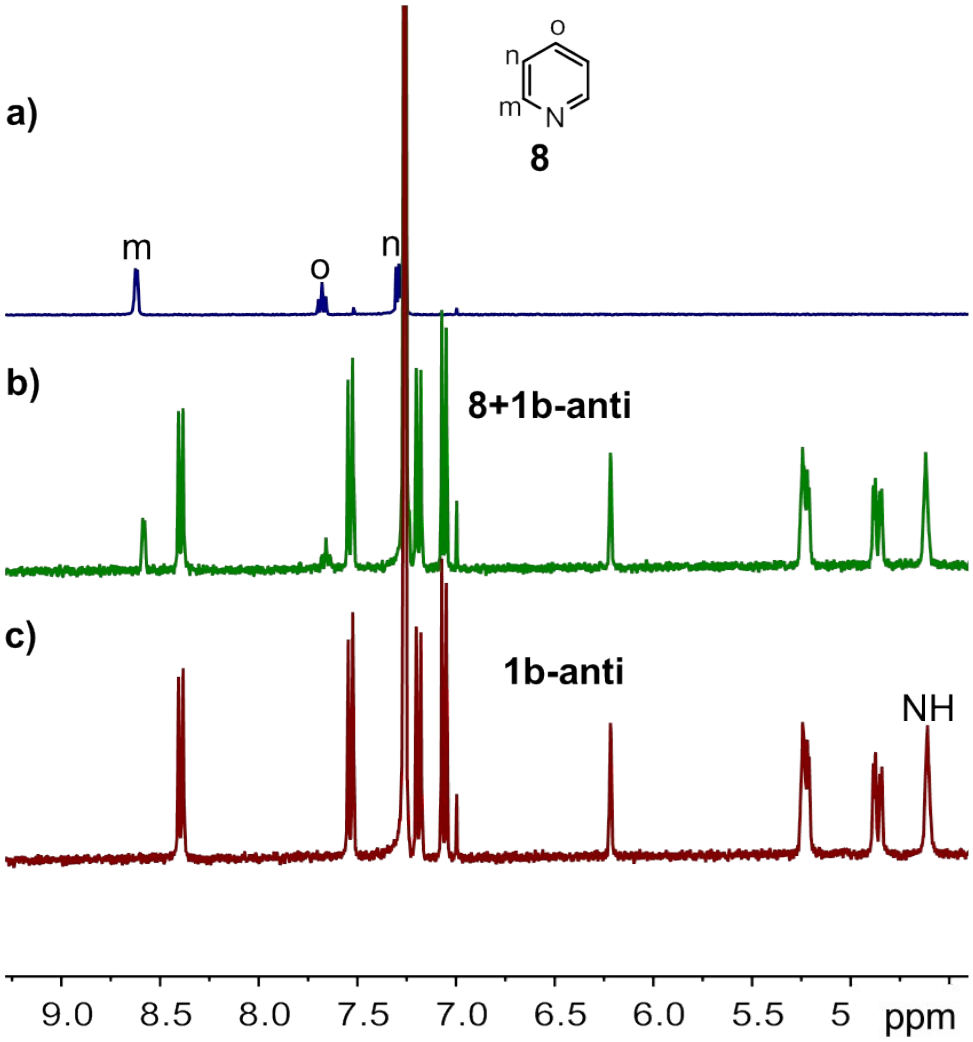

Fig. S18 ^{1}H NMR spectra (400 MHz, $CDCl_3$, 25 ^{o}C) of (a) guest **8**, (c) **1b-anti**, and (b) its equimolar mixture. No obvious change on NH protons was observed, the protons *m, n* and *o* of the guest undergo no shift at all, suggesting very weak binding between **1b-anti** and guest **8**.

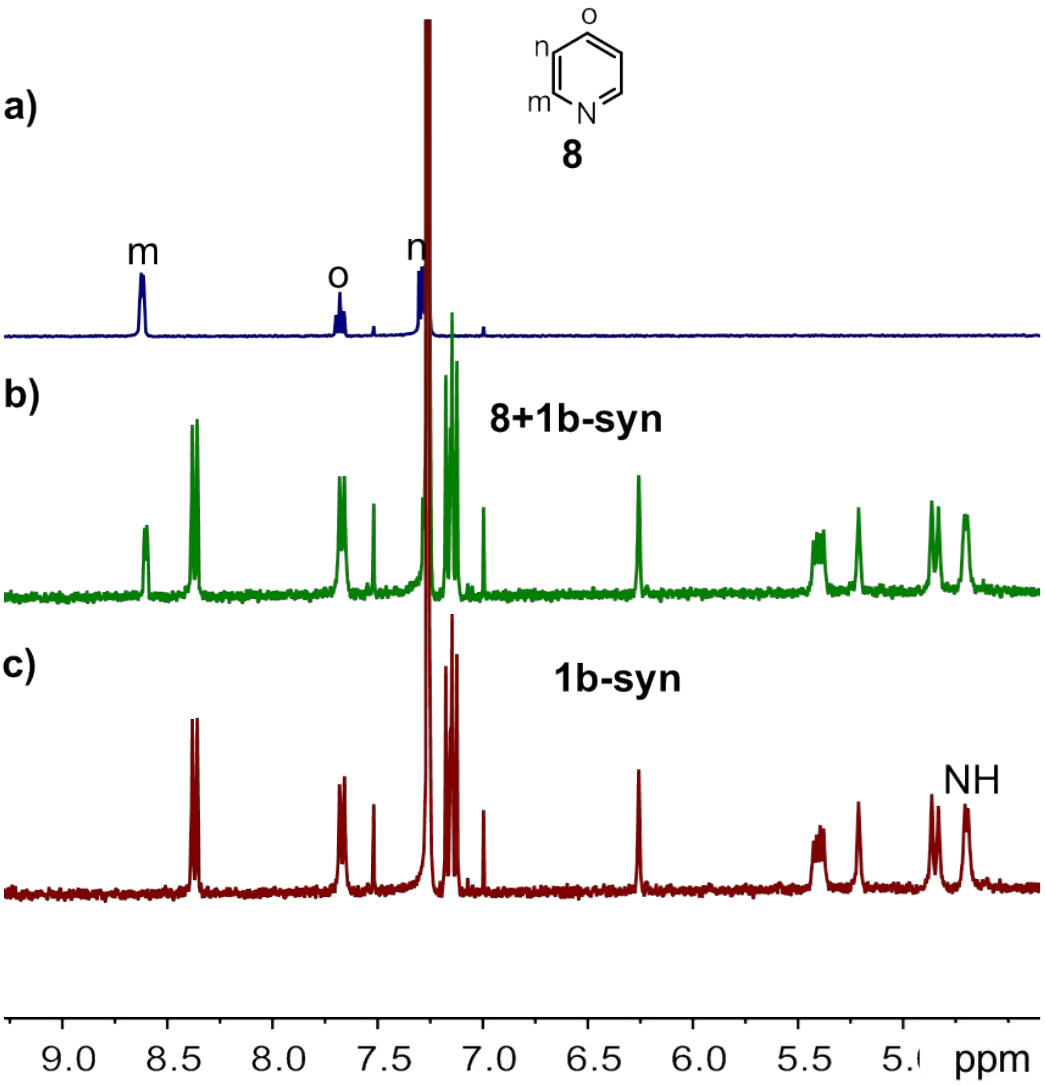

Fig. S19 ^{1}H NMR spectra (400 MHz, $CDCl_3$, 25 ^{o}C) of (a) guest **8**, (c) **1b-syn**, and (b) its equimolar mixture. No obvious change on NH protons was observed, the protons *m, n* and *o* of the guest undergo no shift at all, suggesting very weak binding between **1b-syn** and guest **8**.

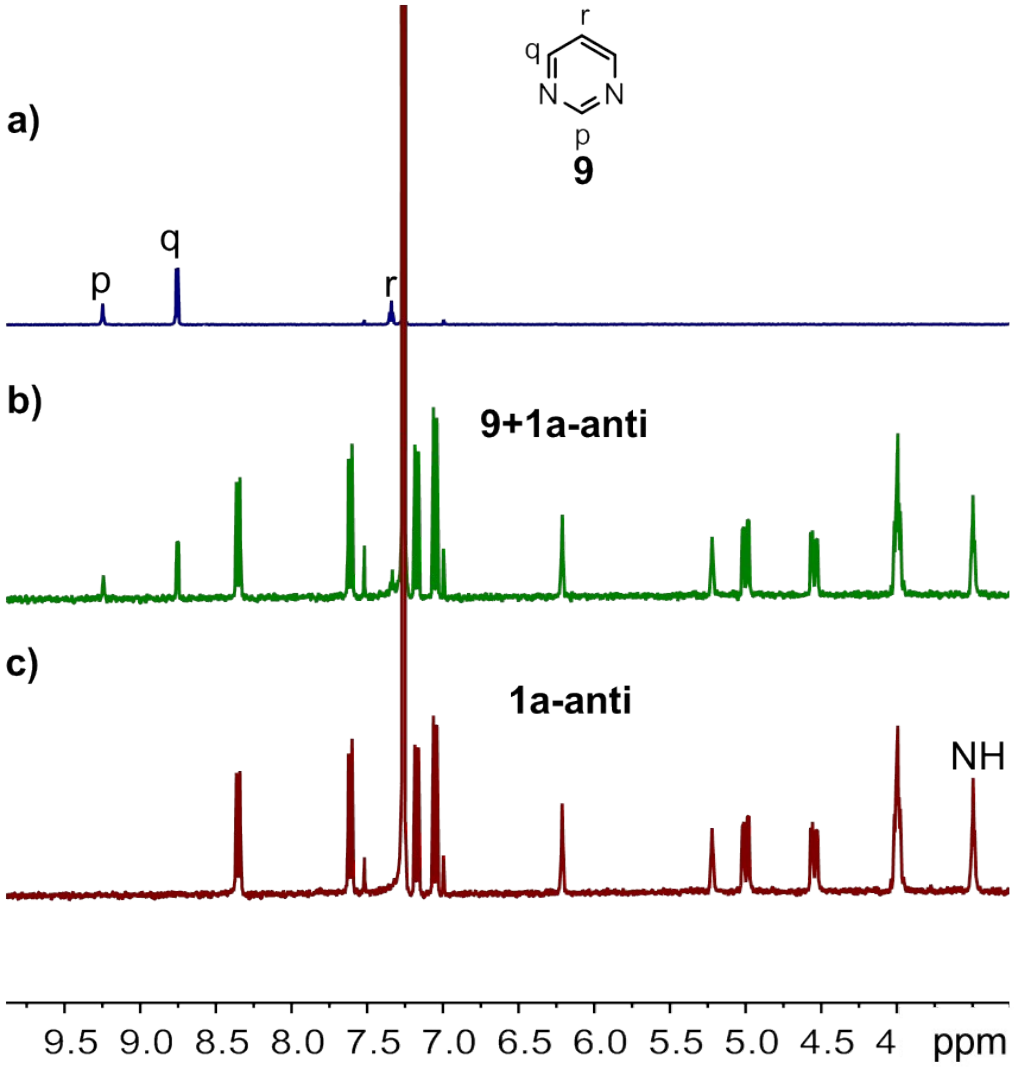

Fig. S20 ^{1}H NMR spectra (400 MHz, $CDCl_3$, 25 ^{o}C) of (a) guest **9**, (c) **1a-anti**, and (b) its equimolar mixture. No obvious change on NH protons was observed, the protons *p, q* and *r* of the guest undergo no shift at all, suggesting very weak binding between **1a-anti** and guest **9**.

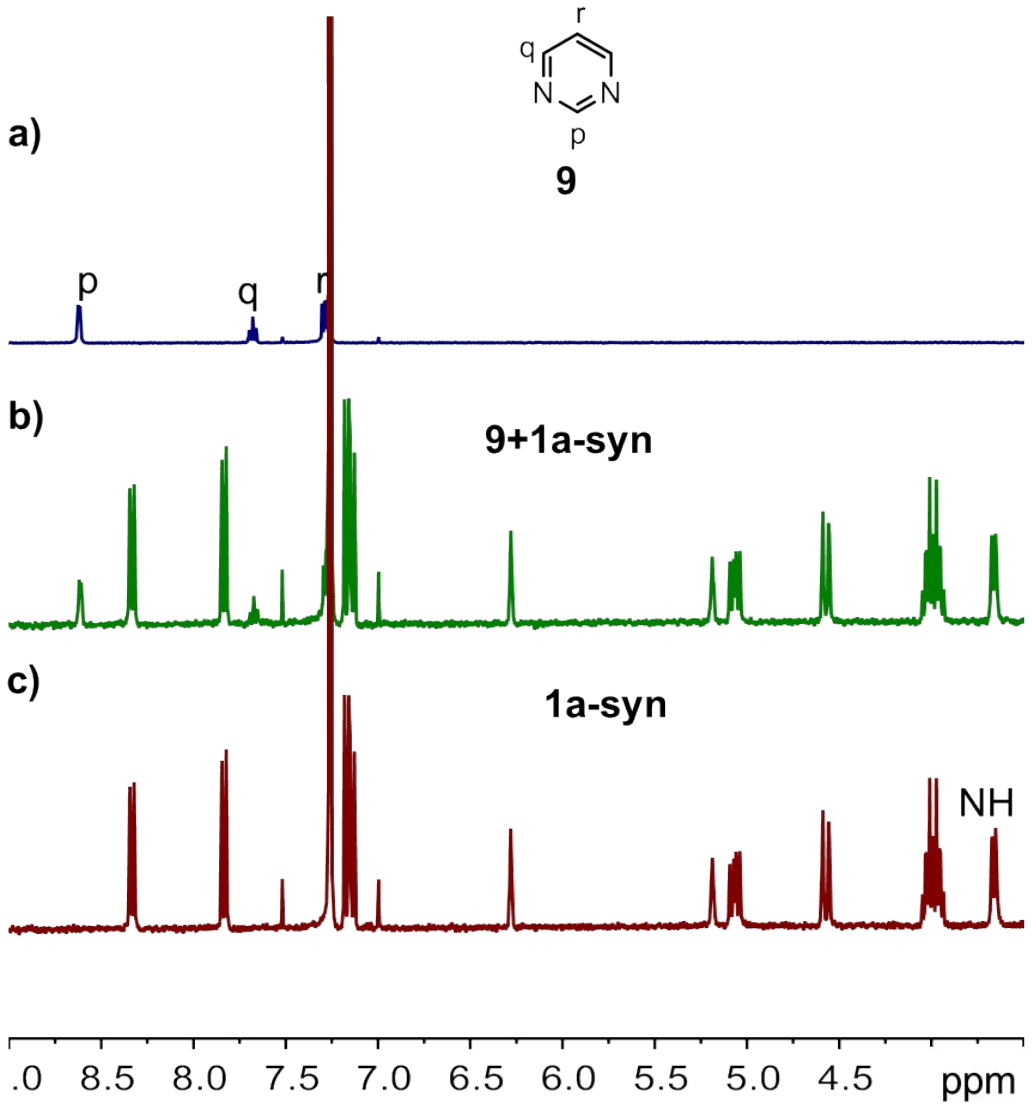

Fig. S21 ^{1}H NMR spectra (400 MHz, $CDCl_3$, 25 ^{o}C) of (a) guest **9**, (c) **1a-syn**, and (b) its equimolar mixture. No obvious change on NH protons was observed, the protons *p, q* and *r* of the guest undergo no shift at all, suggesting very weak binding between **1a-syn** and guest **9**.

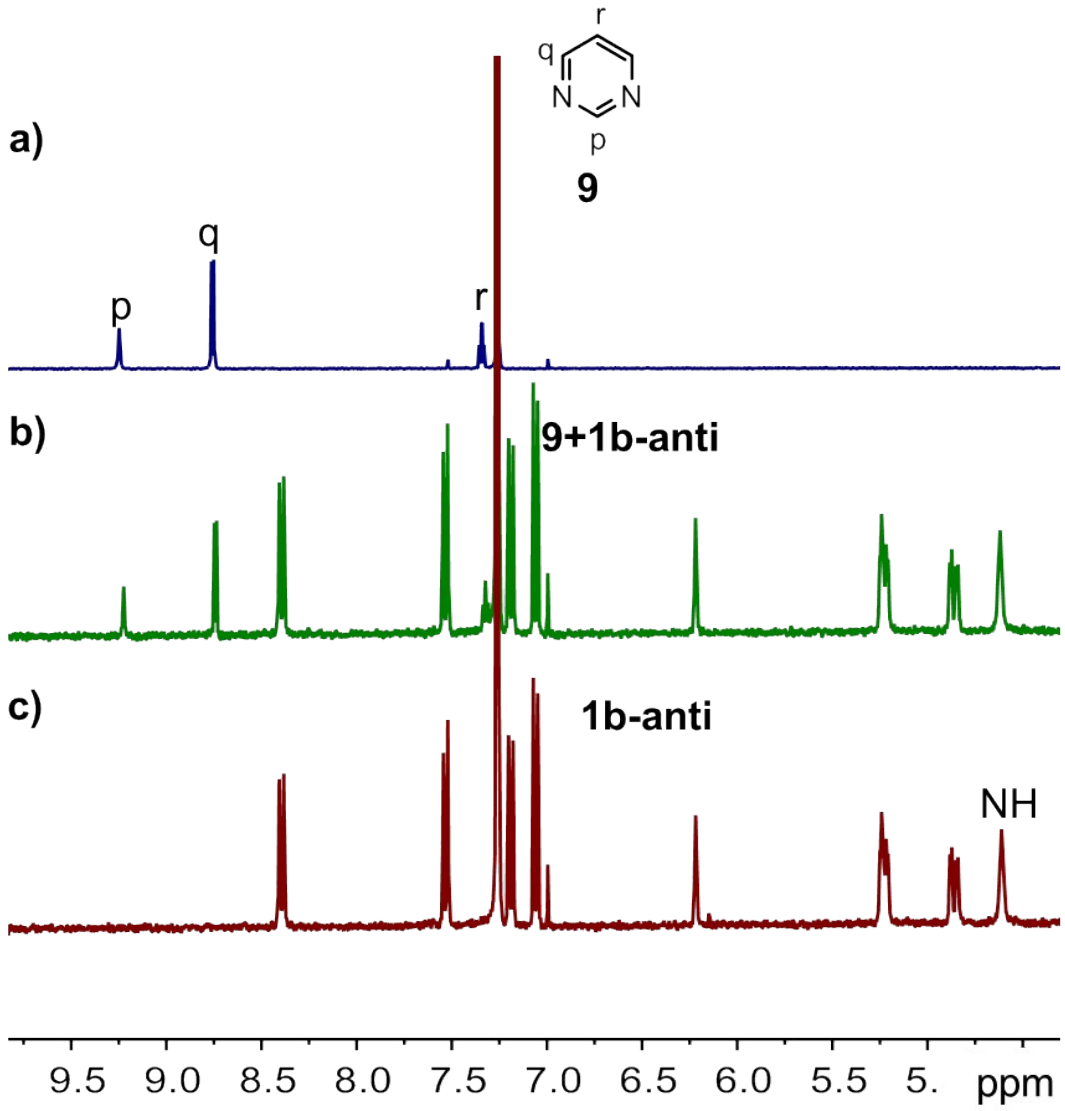

Fig. S22 ^{1}H NMR spectra (400 MHz, $CDCl_3$, 25 ^{o}C) of (a) guest **9**, (c) **1b-anti**, and (b) its equimolar mixture. No obvious change on NH protons was observed, the protons *p, q* and *r* of the guest undergo no shift at all, suggesting very weak binding between **1b-anti** and guest **9**.

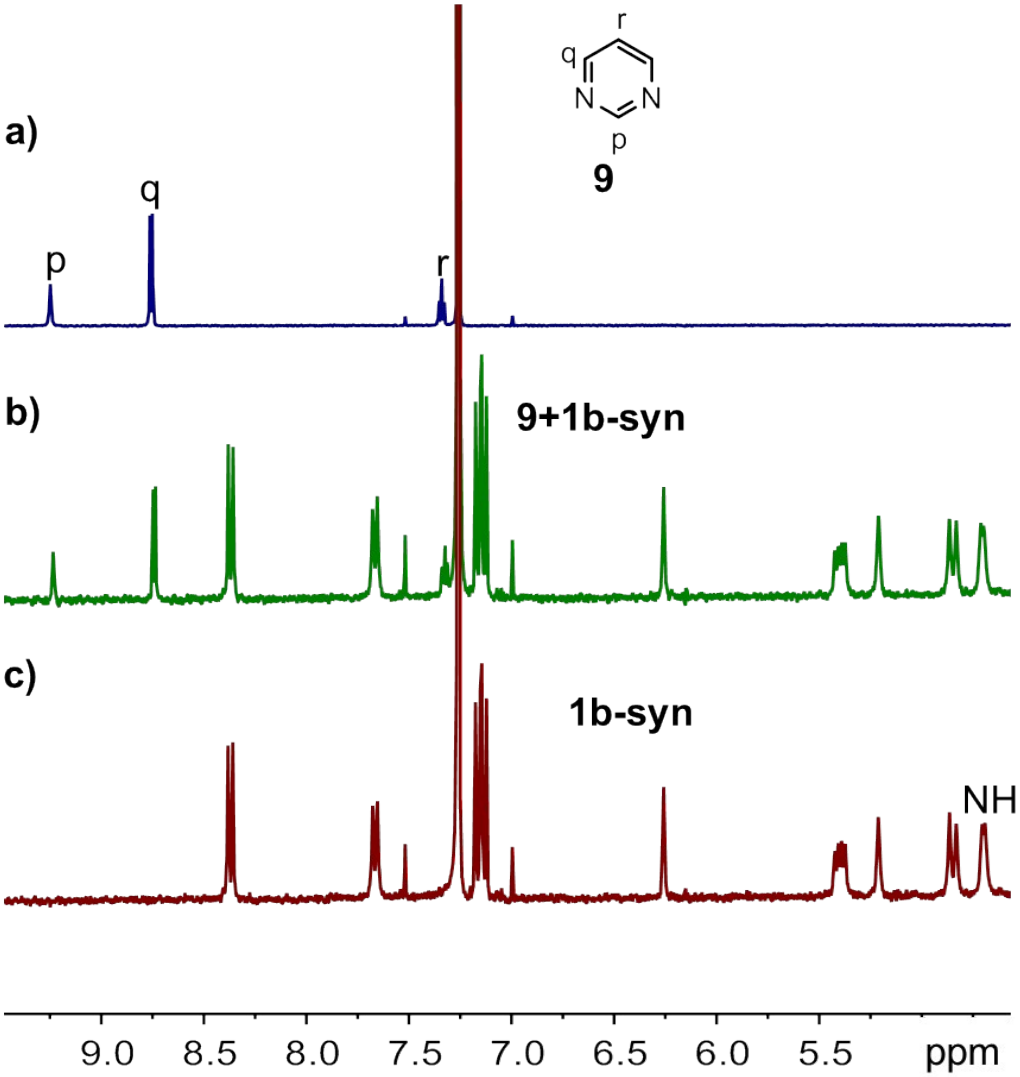

Fig. S23 ^{1}H NMR spectra (400 MHz, $CDCl_3$, 25 ^{o}C) of (a) guest **9**, (c) **1b-syn**, and (b) its equimolar mixture. No obvious change on NH protons was observed, the protons *p, q* and *r* of the guest undergo no shift at all, suggesting very weak binding between **1b-syn** and guest **9**.

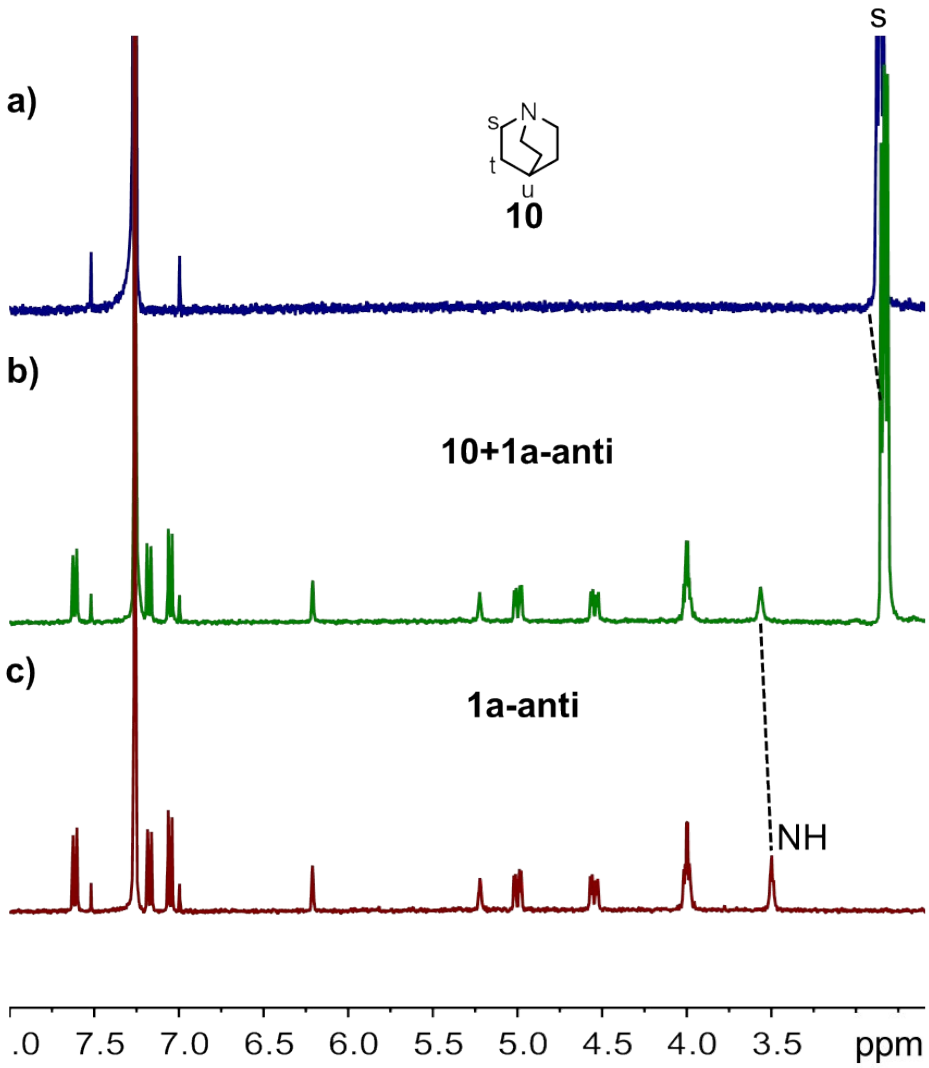

Fig. S24 ^{1}H NMR spectra (400 MHz, $CDCl_3$, 25 ^{o}C) of (a) guest **10**, (c) **1a-anti**, and (b) its equimolar mixture. The protons *s* of the guest experiences the upfield shift, the proton NH of the host experiences the downfield shift, suggesting that the complexation between **1a-anti** and guest **10**.

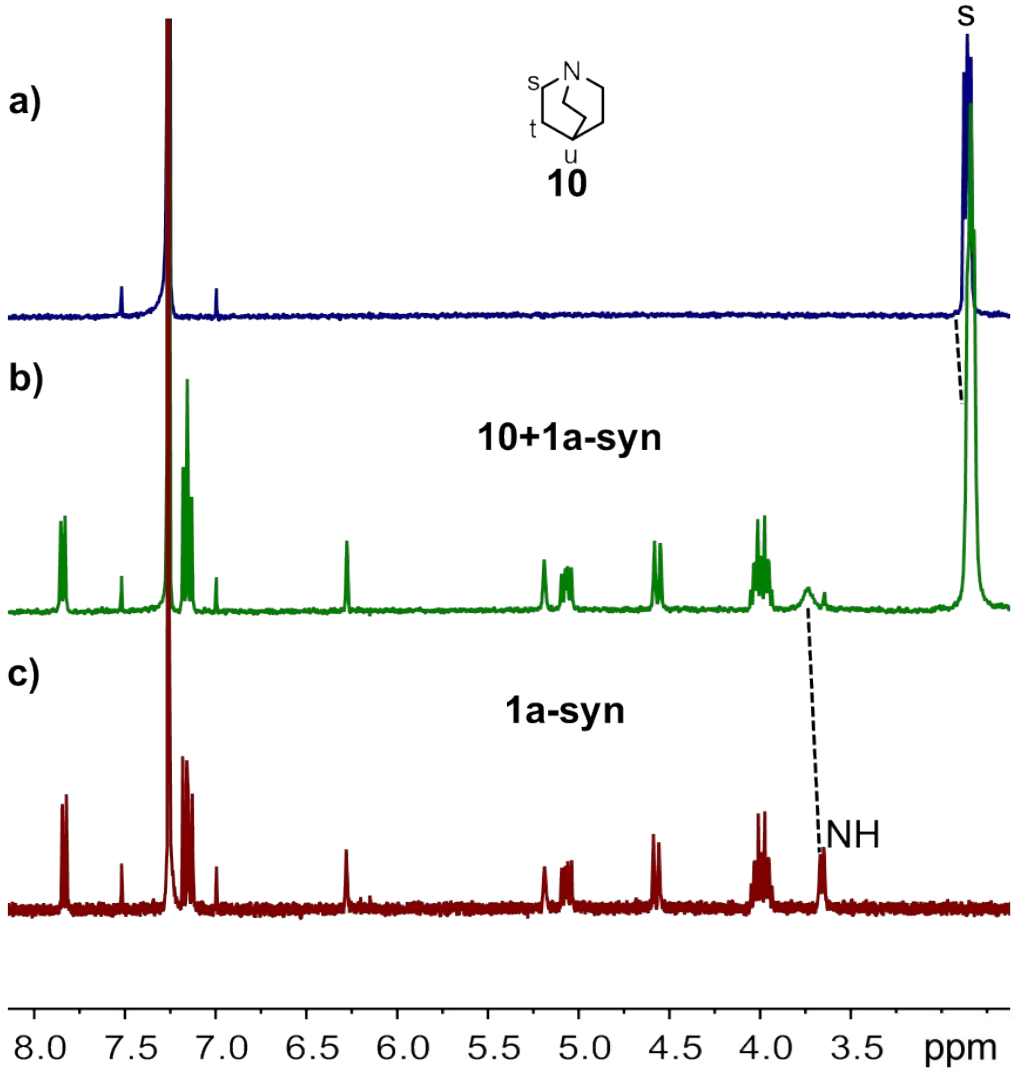

Fig. S25 ^{1}H NMR spectra (400 MHz, $CDCl_3$, 25 ^{o}C) of (a) guest **10**, (c) **1a-syn**, and (b) its equimolar mixture. The protons *s* of the guest experiences the upfield shift, the proton NH of the host experiences the downfield shift, suggesting that the complexation between **1a-syn** and guest **10**.

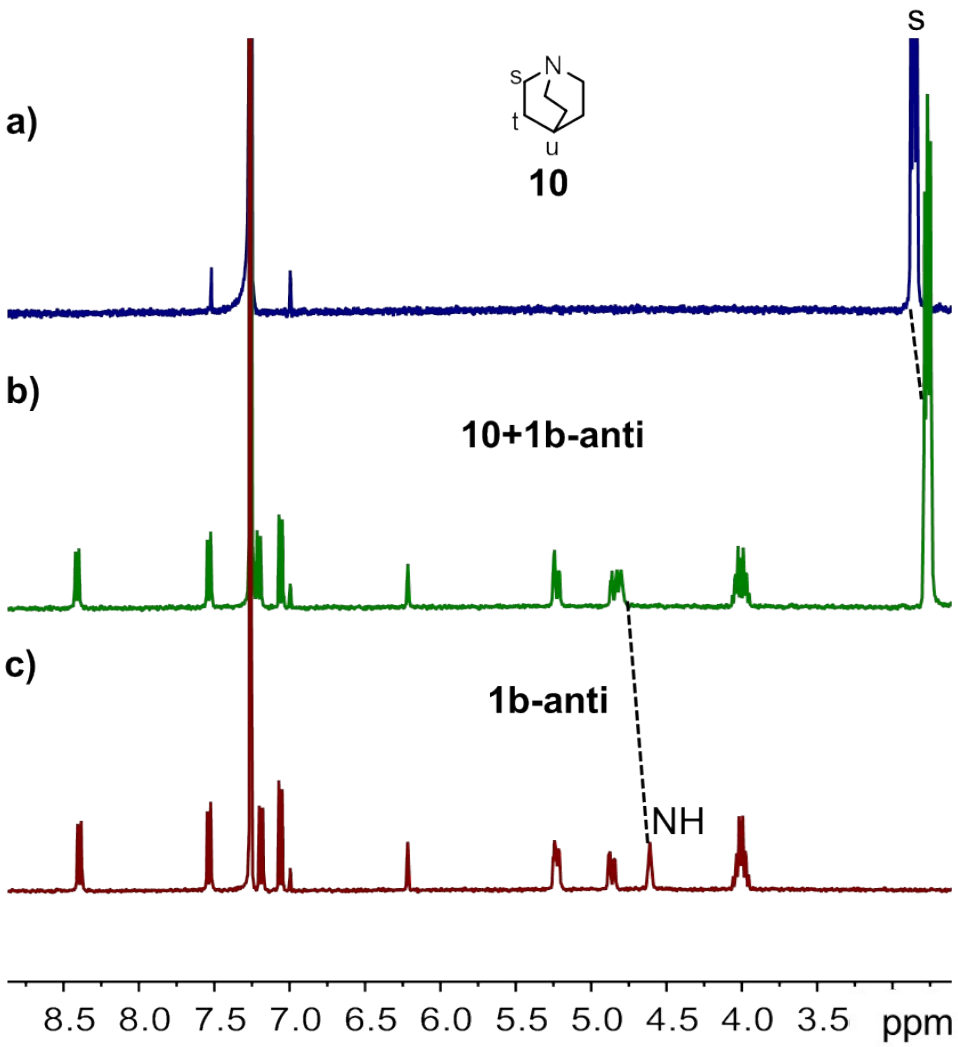

Fig. S26 ^{1}H NMR spectra (400 MHz, $CDCl_3$, 25 ^{o}C) of (a) guest **10**, (c) **1b-anti**, and (b) its equimolar mixture. The protons *s* of the guest experiences the upfield shift, the proton NH of the host experiences the downfield shift, suggesting that the complexation between **1b-anti** and guest **10**.

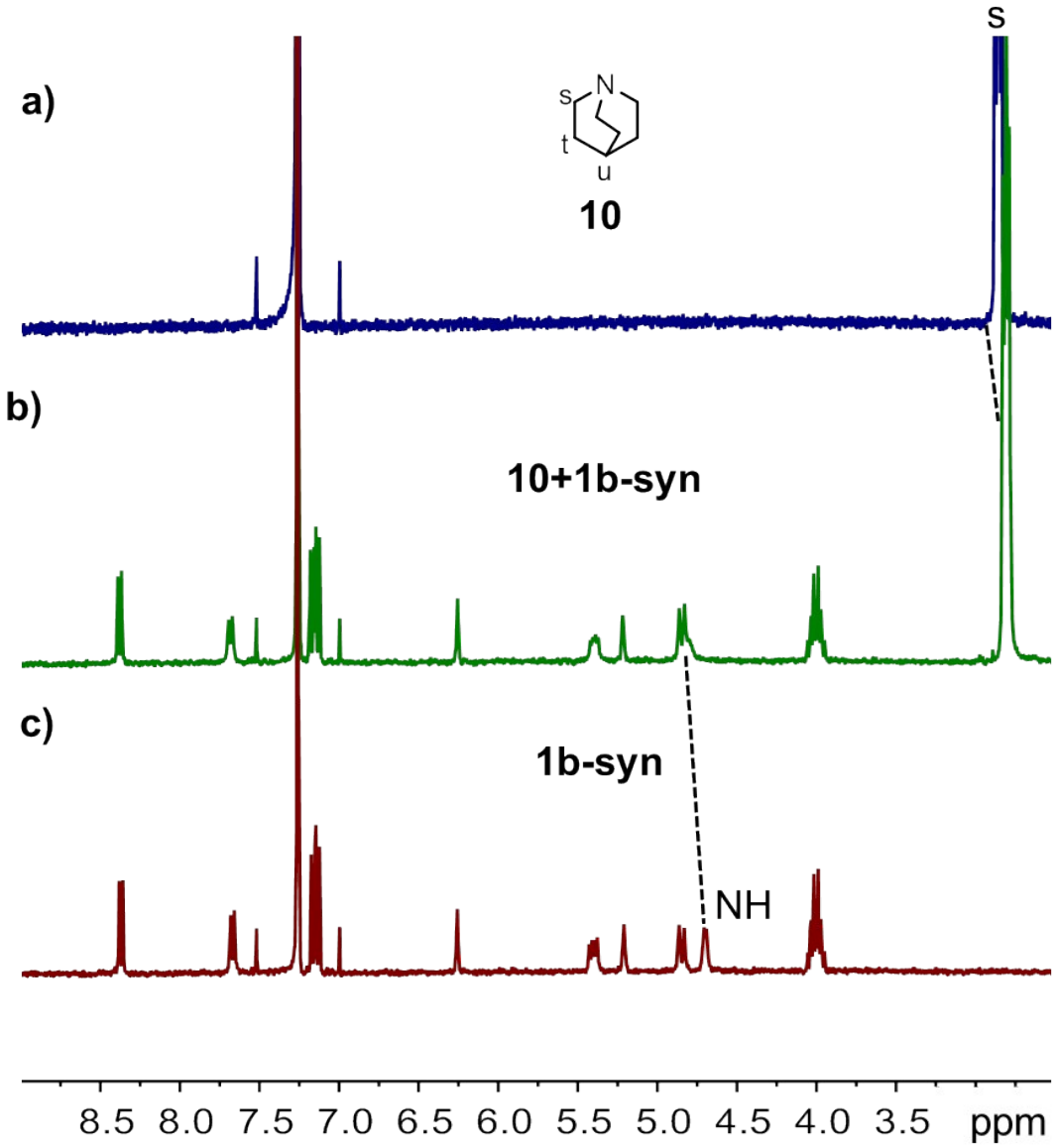

Fig. S27 ^{1}H NMR spectra (400 MHz, $CDCl_3$, 25 ^{o}C) of (a) guest **10**, (c) **1b-syn**, and (b) its equimolar mixture. The protons *s* of the guest experiences the upfield shift, the proton NH of the host experiences the downfield shift, suggesting that the complexation between **1b-syn** and guest **10**.

5. Determination of Binding Constants.

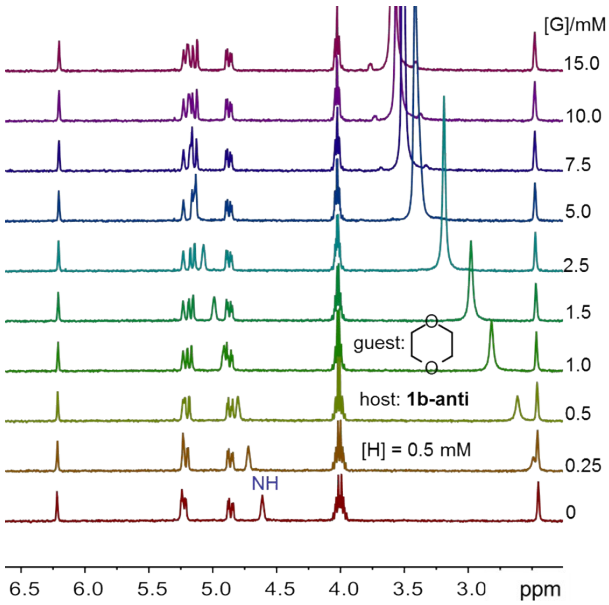

Fig. S28 Partial ^{1}H NMR spectra (400 MHz, $CDCl_3$, 25 ^oC) of **1b-anti** (0.5 mM) titrated by the guest **2** (0~15.0 mM). The nonlinear curve-fitting method and 1:1 binding stoichiometry as reported before[6] were used to obtain the association constants.

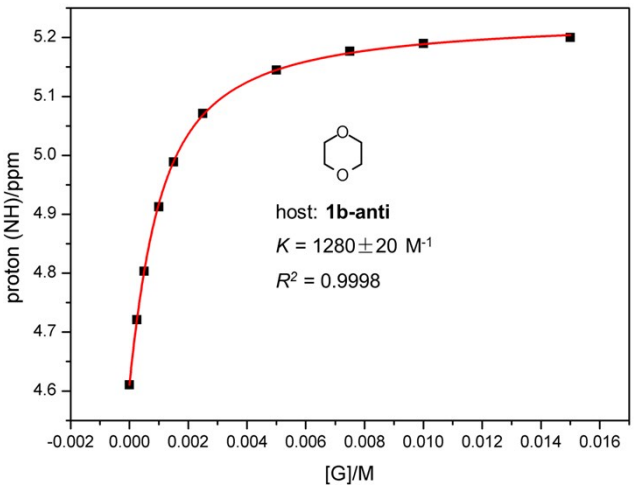

Fig. S29 Non-linear curve-fitting for the complexation between **1b-anti** and the guest **2** in $CDCl_3$ at 25 ^oC. The chemical shifts of proton NH was monitored during the titration for the calculation of binding constants. This is the same for all the following experiments, unless otherwise noted.

---

6 G. Huang, Z. He, C. Cai, F. Pan, D. Yang, K. Rissanen and W Jiang. *Chem. Commun.*, 2015, **51**, 15490-15493.

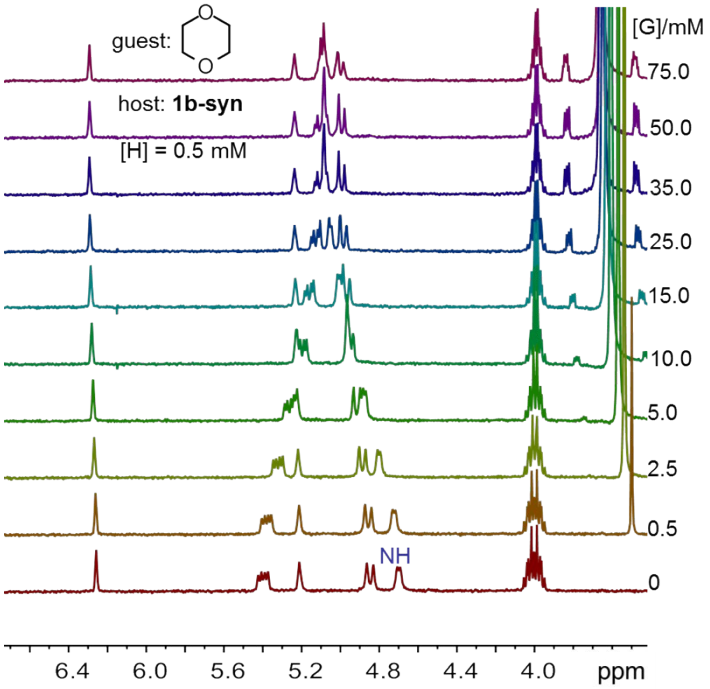

Fig. S30 Partial ^{1}H NMR spectra (400 MHz, $CDCl_3$, 25 ^oC) of **1b-syn** (0.5 mM) titrated by the guest **2** (0~75.0 mM).

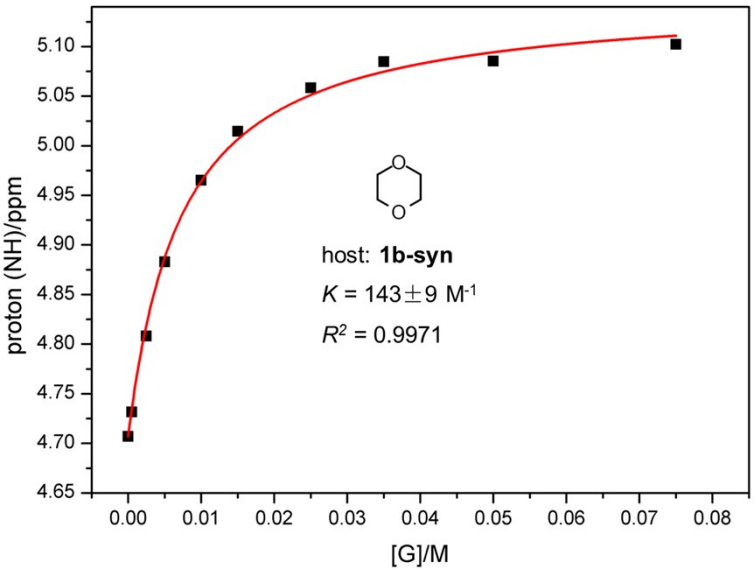

Fig. S31 Non-linear curve-fitting for the complexation between **1b-syn** and the guest **2** in $CDCl_3$ at 25 ^oC.

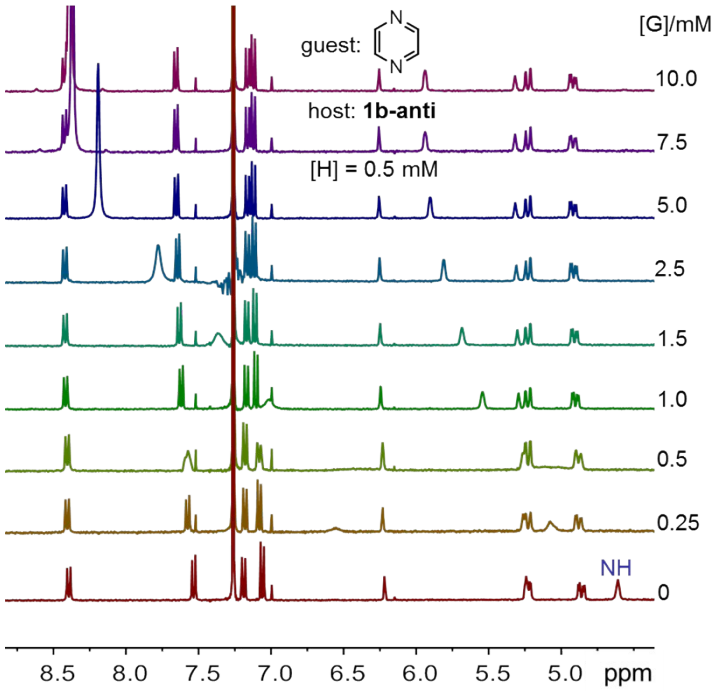

Fig. S32 Partial ^{1}H NMR spectra (400 MHz, $CDCl_3$, 25 ^{o}C) of **1b-anti** (0.5 mM) titrated by the guest **3** (0~10.0 mM).

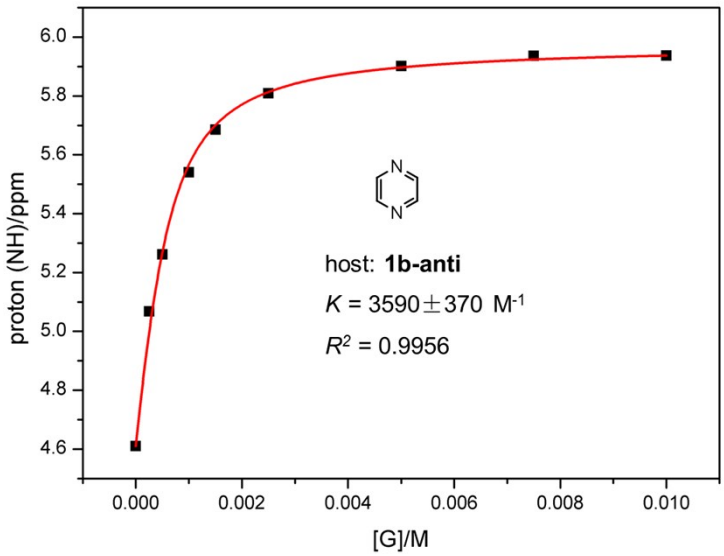

Fig. S33 Non-linear curve-fitting for the complexation between **1b-anti** and the guest **3** in $CDCl_3$ at 25 ^{o}C.

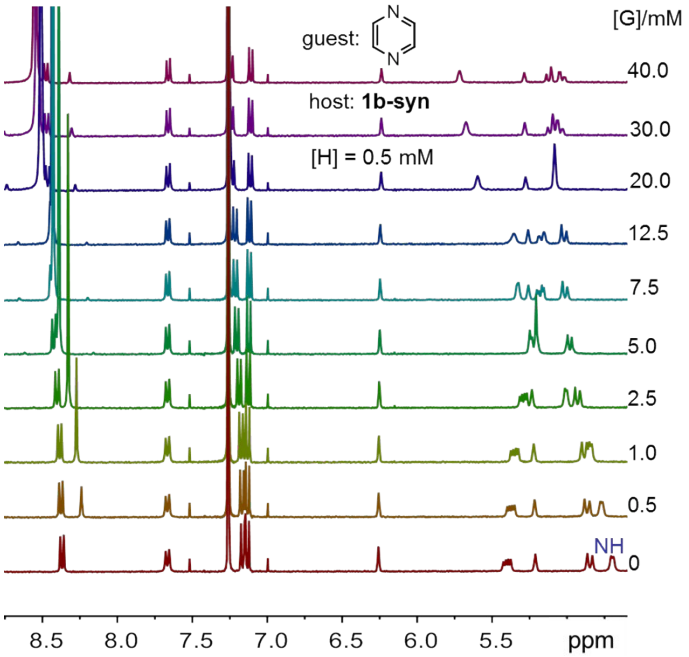

Fig. S34 Partial ^{1}H NMR spectra (400 MHz, $CDCl_3$, 25 ^oC) of **1b-syn** (0.5 mM) titrated by the guest **3** (0~40.0 mM).

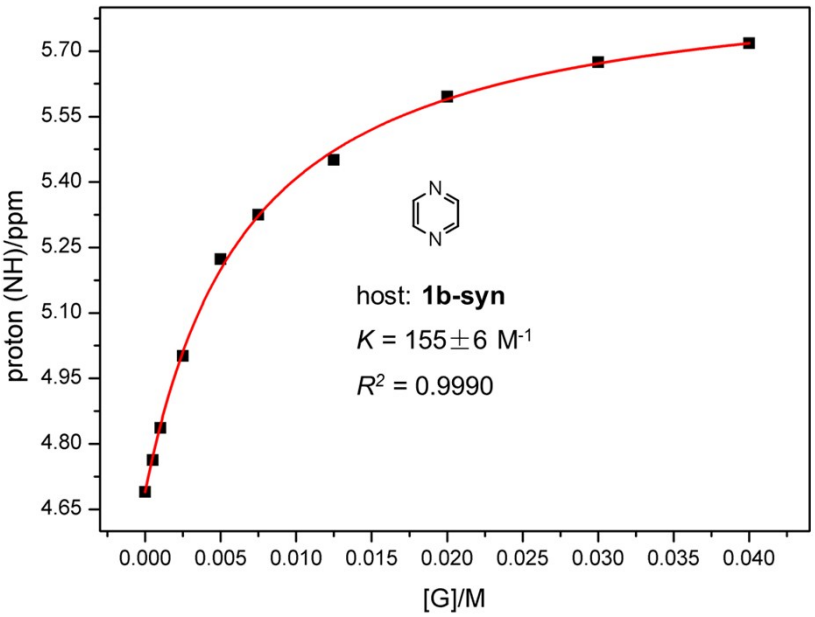

Fig. S35 Non-linear curve-fitting for the complexation between **1b-syn** and the guest **3** in $CDCl_3$ at 25 ^oC.

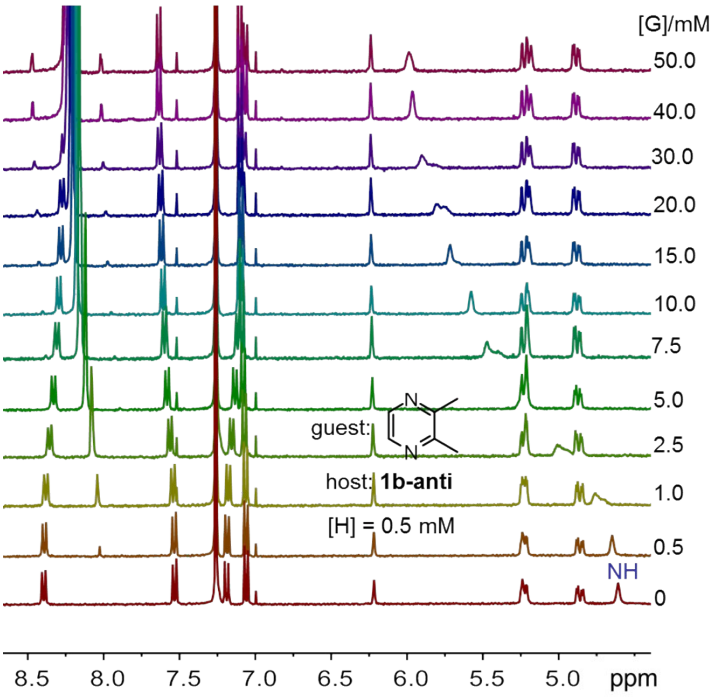

Fig. S36 Partial ^{1}H NMR spectra (400 MHz, $CDCl_3$, 25 ^oC) of **1b-anti** (0.5 mM) titrated by the guest **4** (0~50.0 mM).

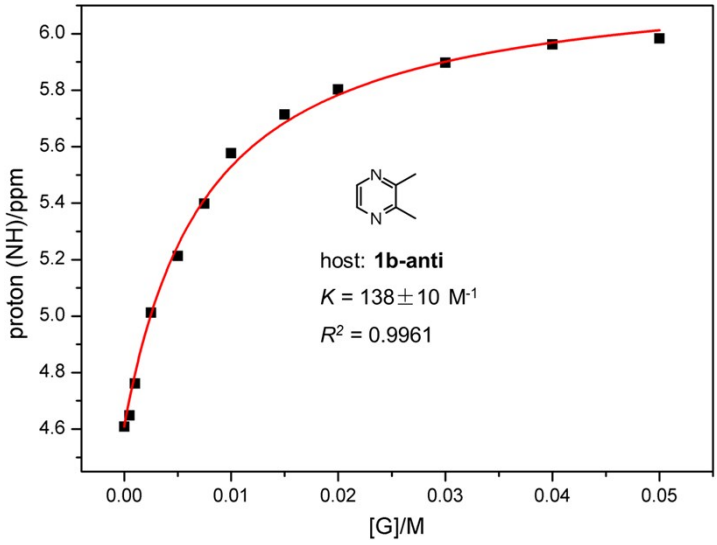

Fig. S37 Non-linear curve-fitting for the complexation between **1b-anti** and the guest **4** in $CDCl_3$ at 25 ^oC.

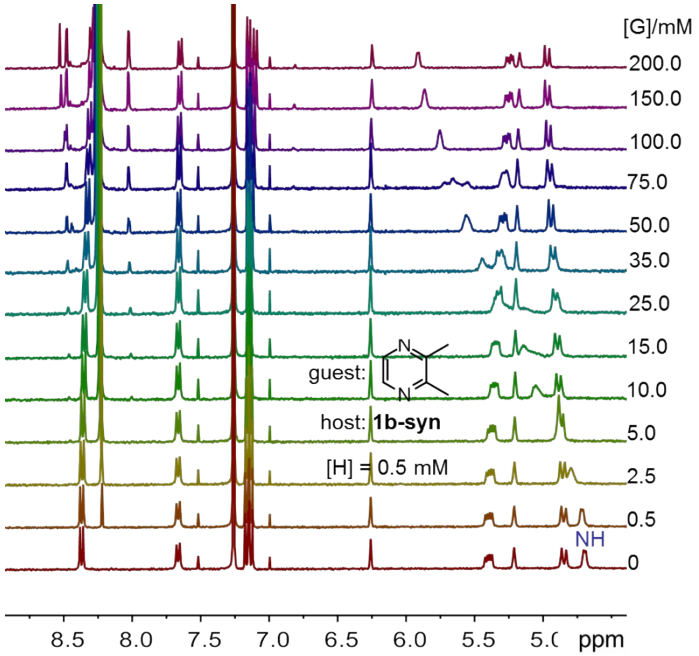

Fig. S38 Partial ^{1}H NMR spectra (400 MHz, $CDCl_3$, 25 ^oC) of **1b-syn** (0.5 mM) titrated by the guest **4** (0~200.0 mM).

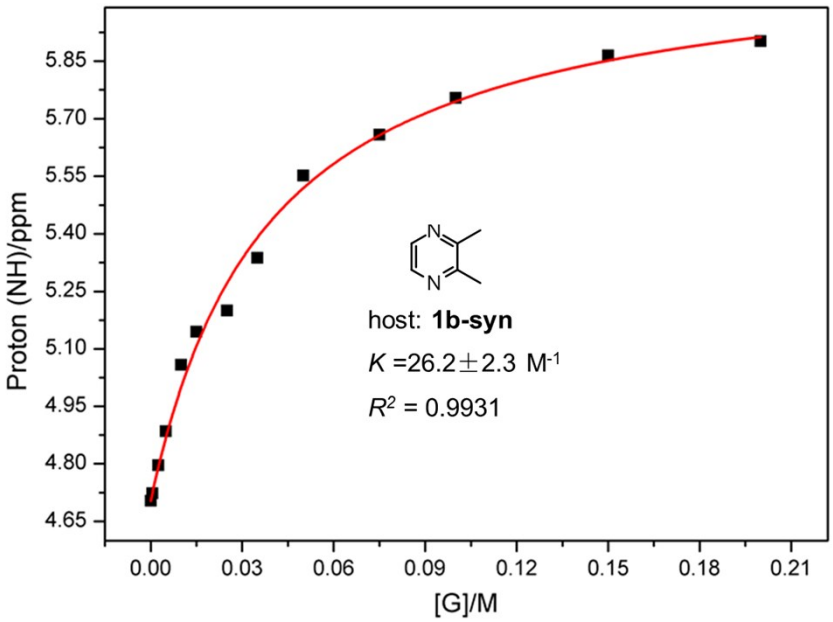

Fig. S39 Non-linear curve-fitting for the complexation between **1b-syn** and the guest **4** in $CDCl_3$ at 25 ^oC.

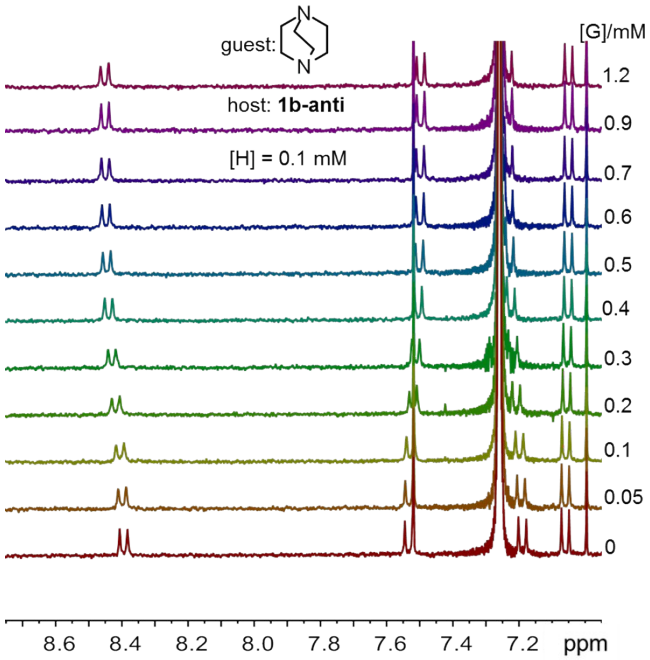

Fig. S40 Partial ^{1}H NMR spectra (400 MHz, $CDCl_3$, 25 ^{o}C) of **1b-anti** (0.1 mM) titrated by the guest **5** (0~1.2 mM). This binding constant is very large. In order to obtain a more reliable data, the concentration of 1b-anti was decreased to 0.1 mM. Even though, a large error was still observed.

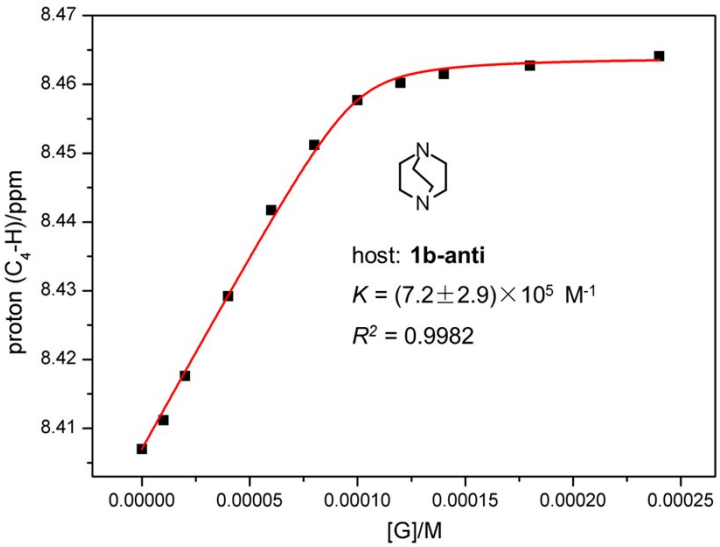

Fig. S41 Non-linear curve-fitting for the complexation between **1b-anti** and the guest **5** in $CDCl_3$ at 25 ^{o}C. Proton 4 was used instead of proton NH since the former can be more clearly monitored during titration.

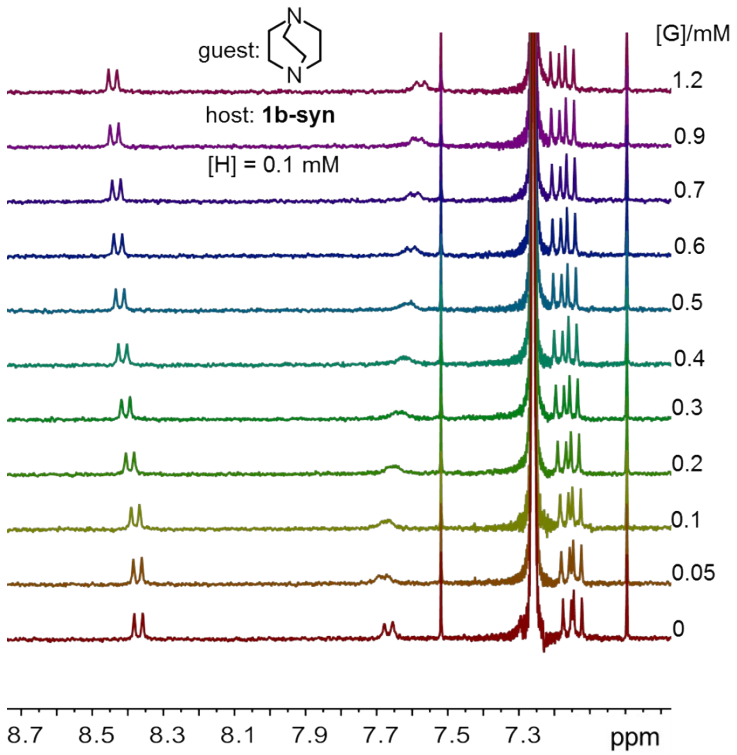

Fig. S42 Partial ^{1}H NMR spectra (400 MHz, $CDCl_3$, 25 ^oC) of **1b-syn** (0.1 mM) titrated by the guest **5** (0~1.2 mM).

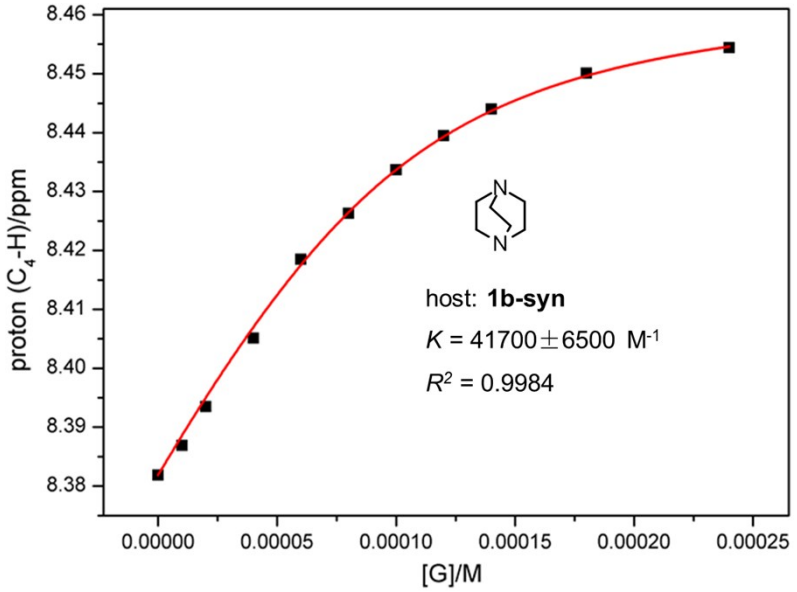

Fig. S43 Non-linear curve-fitting for the complexation between **1b-syn** and the guest **5** in $CDCl_3$ at 25 ^oC.

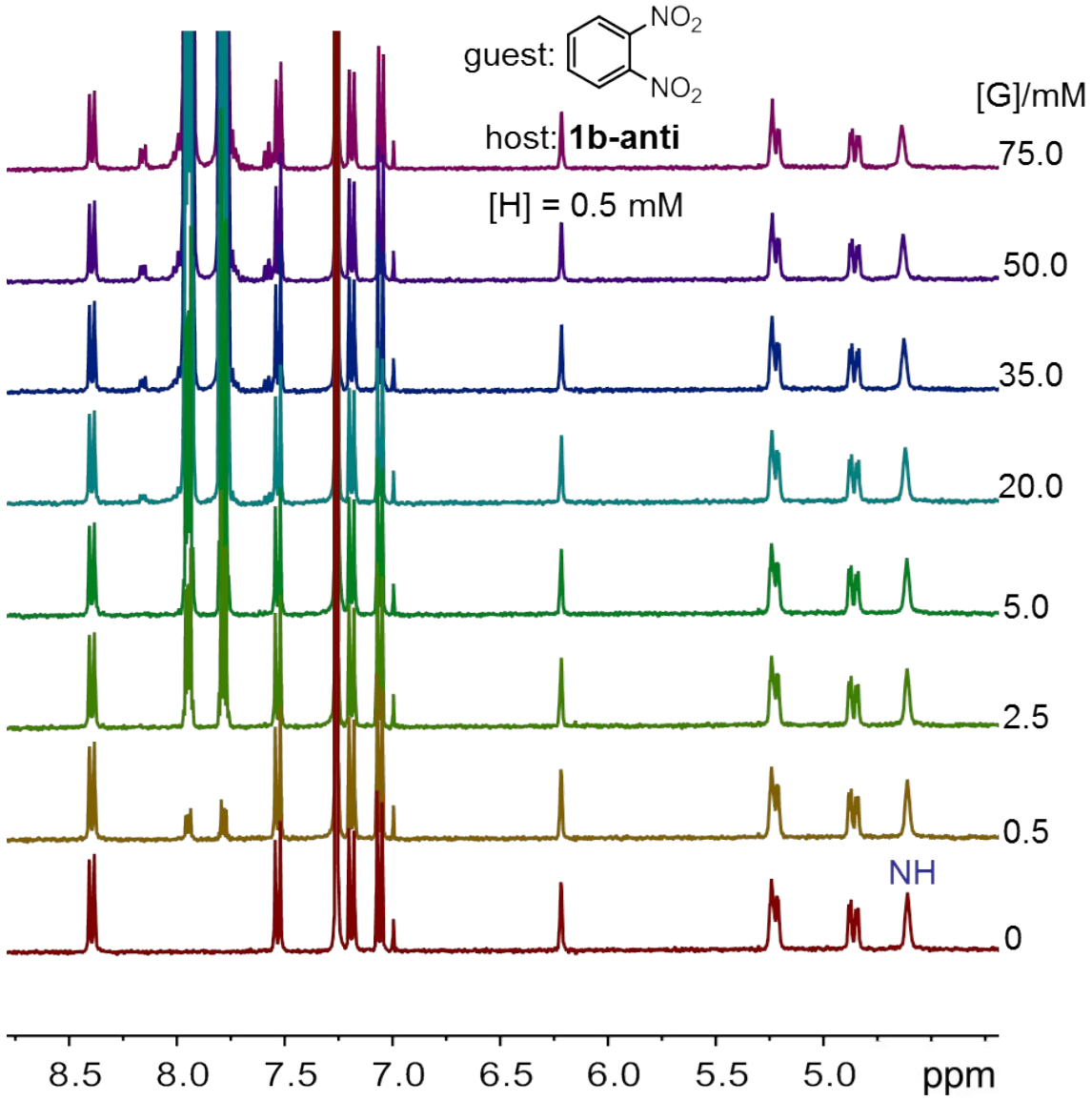

Fig. S44 Partial ^{1}H NMR spectra (400 MHz, $CDCl_3$, 25 ^{o}C) of **1b-anti** (0.5 mM) titrated by the guest **6** (0~75.0 mM). No obvious change on the ^{1}H NMR spectra is observed, suggesting very weak binding between **6** and **1b-anti** (likely < 1 M^{-1}).

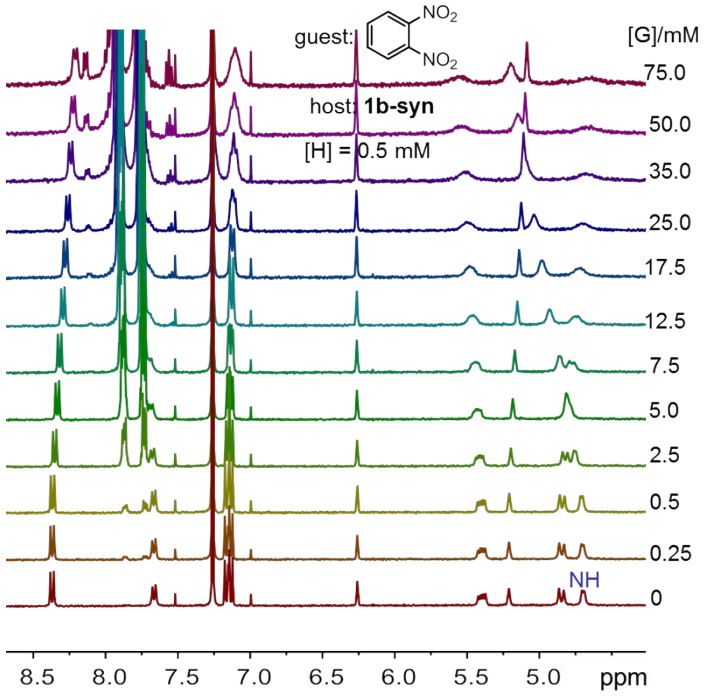

Fig. S45 Partial ^{1}H NMR spectra (400 MHz, $CDCl_3$, 25 ^oC) of **1b-syn** (0.5 mM) titrated by the guest **6** (0~75.0 mM).

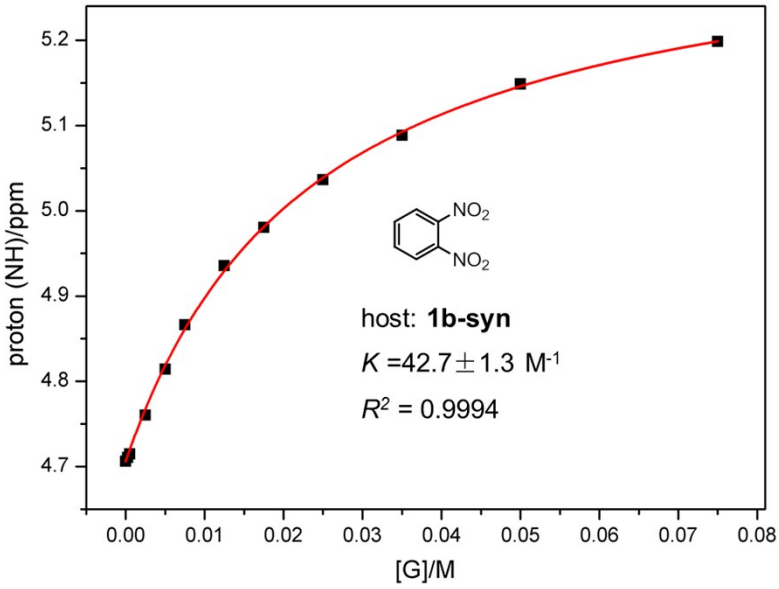

Fig. S46 Non-linear curve-fitting for the complexation between **1b-syn** and the guest **6** in $CDCl_3$ at 25 ^oC.

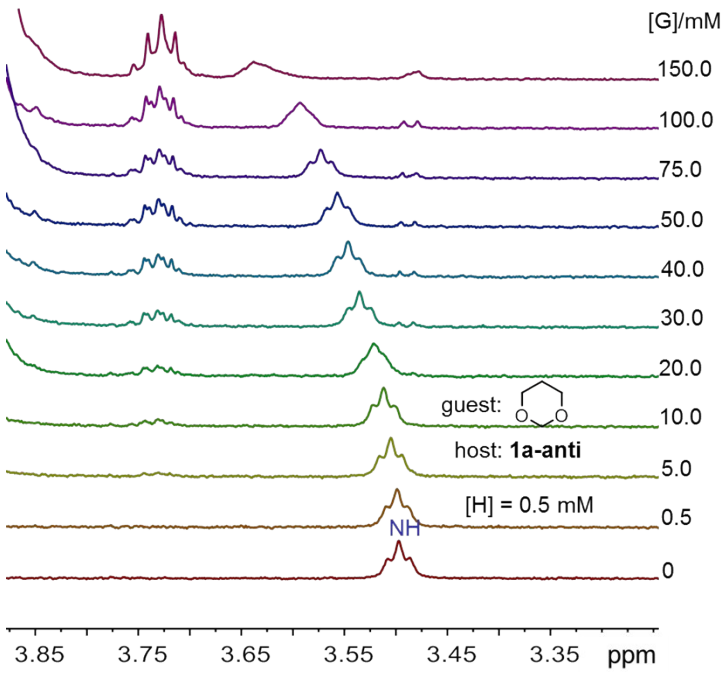

Fig. S47 Partial ^{1}H NMR spectra (400 MHz, $CDCl_3$, 25 ^oC) of **1a-anti** (0.5 mM) titrated by the guest **7** (0~150.0 mM).

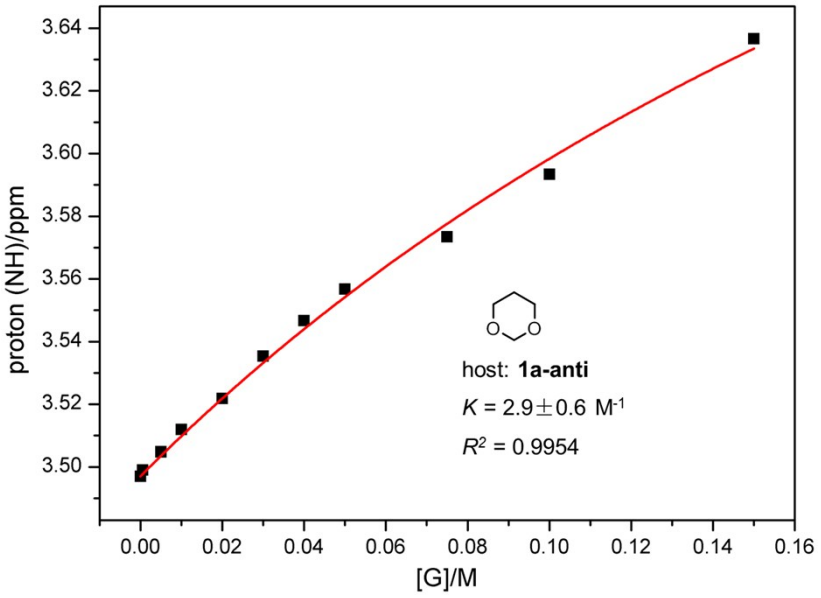

Fig. S48 Non-linear curve-fitting for the complexation between **1a-anti** and the guest **7** in $CDCl_3$ at 25 ^oC.

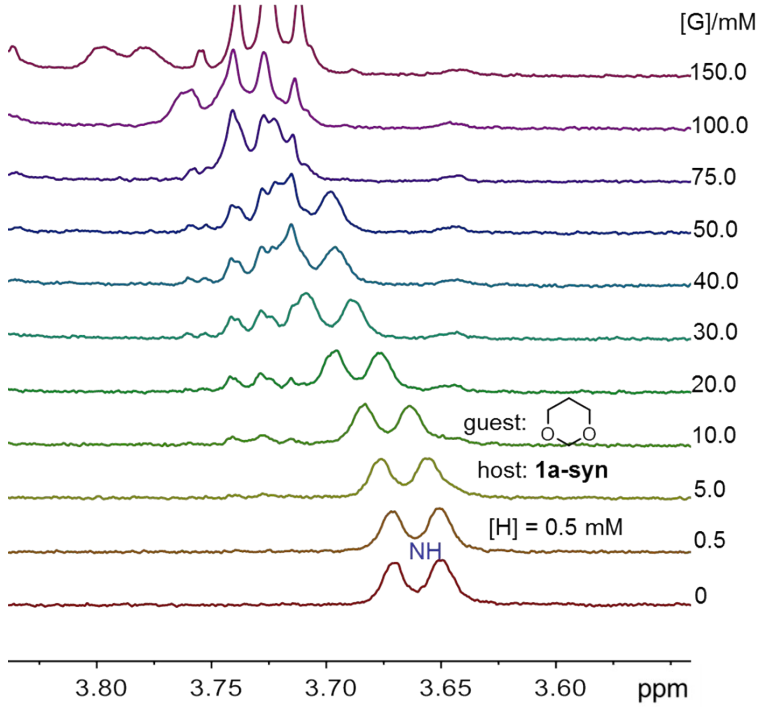

Fig. S49 Partial ^{1}H NMR spectra (400 MHz, $CDCl_3$, 25 ^oC) of **1a-syn** (0.5 mM) titrated by the guest **7** (0~150.0 mM).

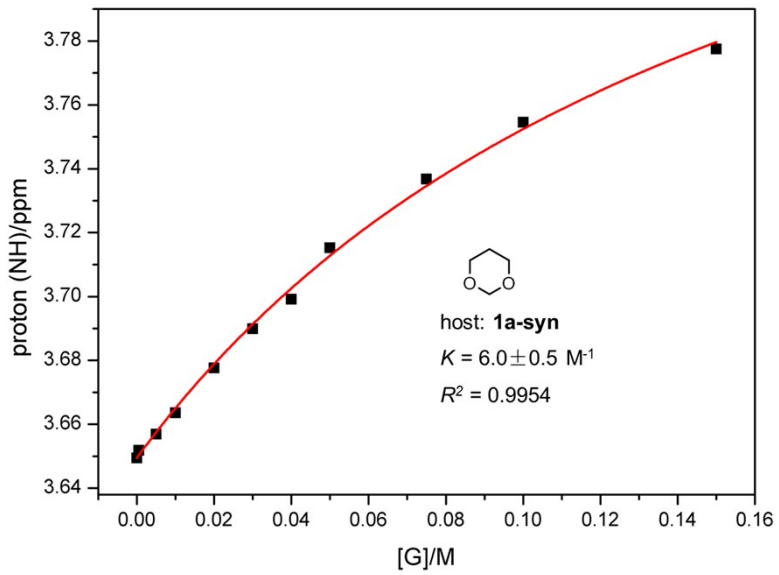

Fig. S50 Non-linear curve-fitting for the complexation between **1a-syn** and the guest **7** in $CDCl_3$ at 25 ^oC.

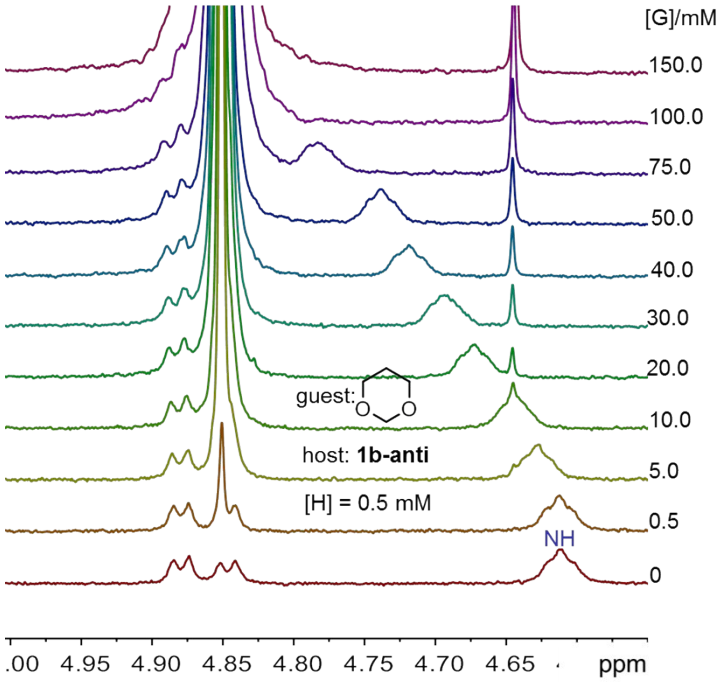

Fig. S51 Partial ^{1}H NMR spectra (400 MHz, $CDCl_3$, 25 ^oC) of **1b-anti** (0.5 mM) titrated by the guest **7** (0~150.0 mM).

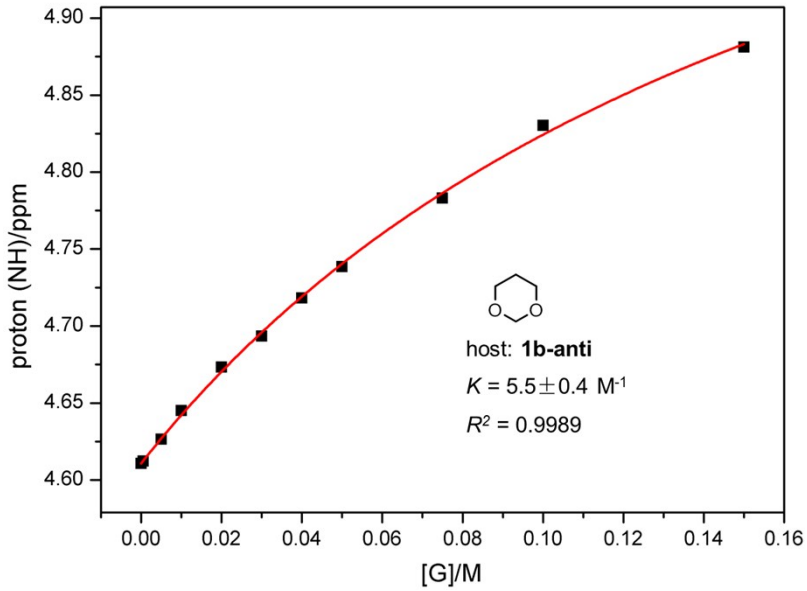

Fig. S52 Non-linear curve-fitting for the complexation between **1b-anti** and the guest **7** in $CDCl_3$ at 25 ^oC.

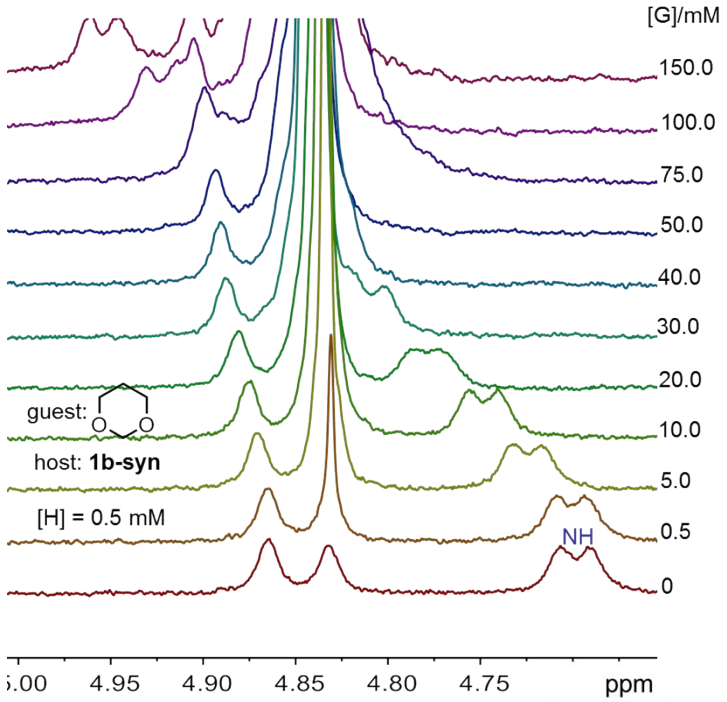

Fig. S53 Partial ^{1}H NMR spectra (400 MHz, $CDCl_3$, 25 ^oC) of **1b-syn** (0.5 mM) titrated by the guest **7** (0~150.0 mM).

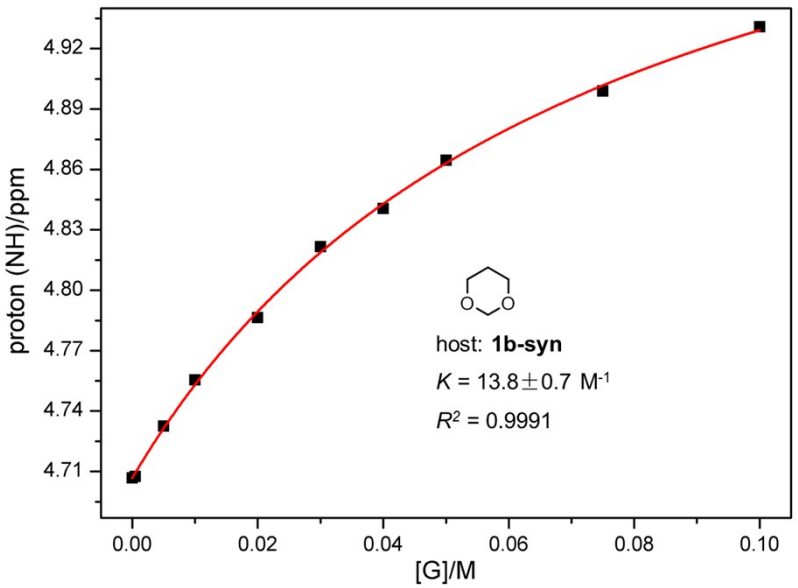

Fig. S54 Non-linear curve-fitting for the complexation between **1b-syn** and the guest **7** in $CDCl_3$ at 25 ^oC.

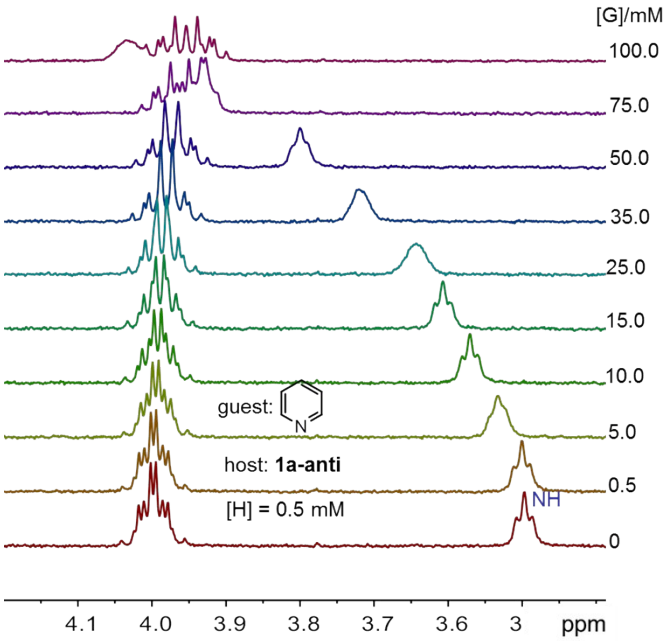

Fig. S55 Partial ^{1}H NMR spectra (400 MHz, $CDCl_3$, 25 ^oC) of **1a-anti** (0.5 mM) titrated by the guest **8** (0~100.0 mM).

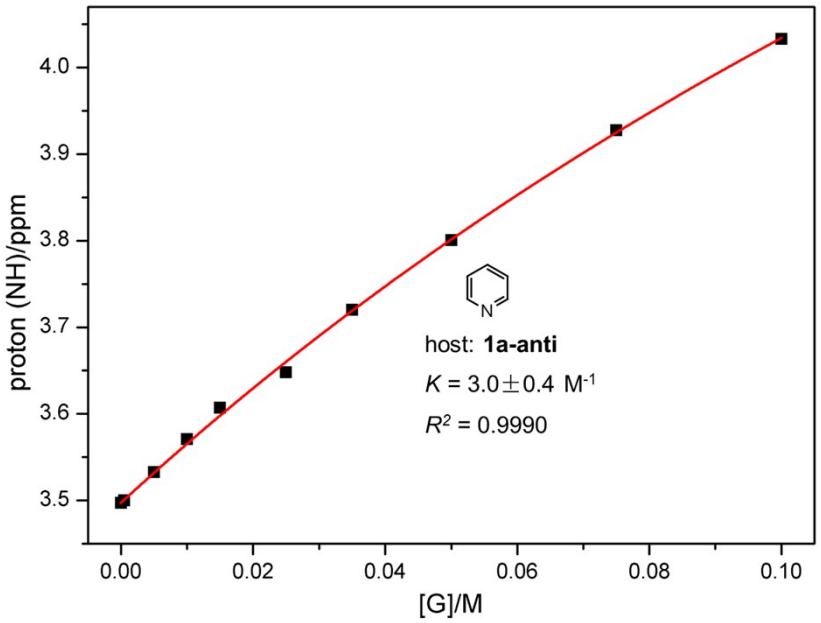

Fig. S56 Non-linear curve-fitting for the complexation between **1a-anti** and the guest **8** in $CDCl_3$ at 25 ^oC.

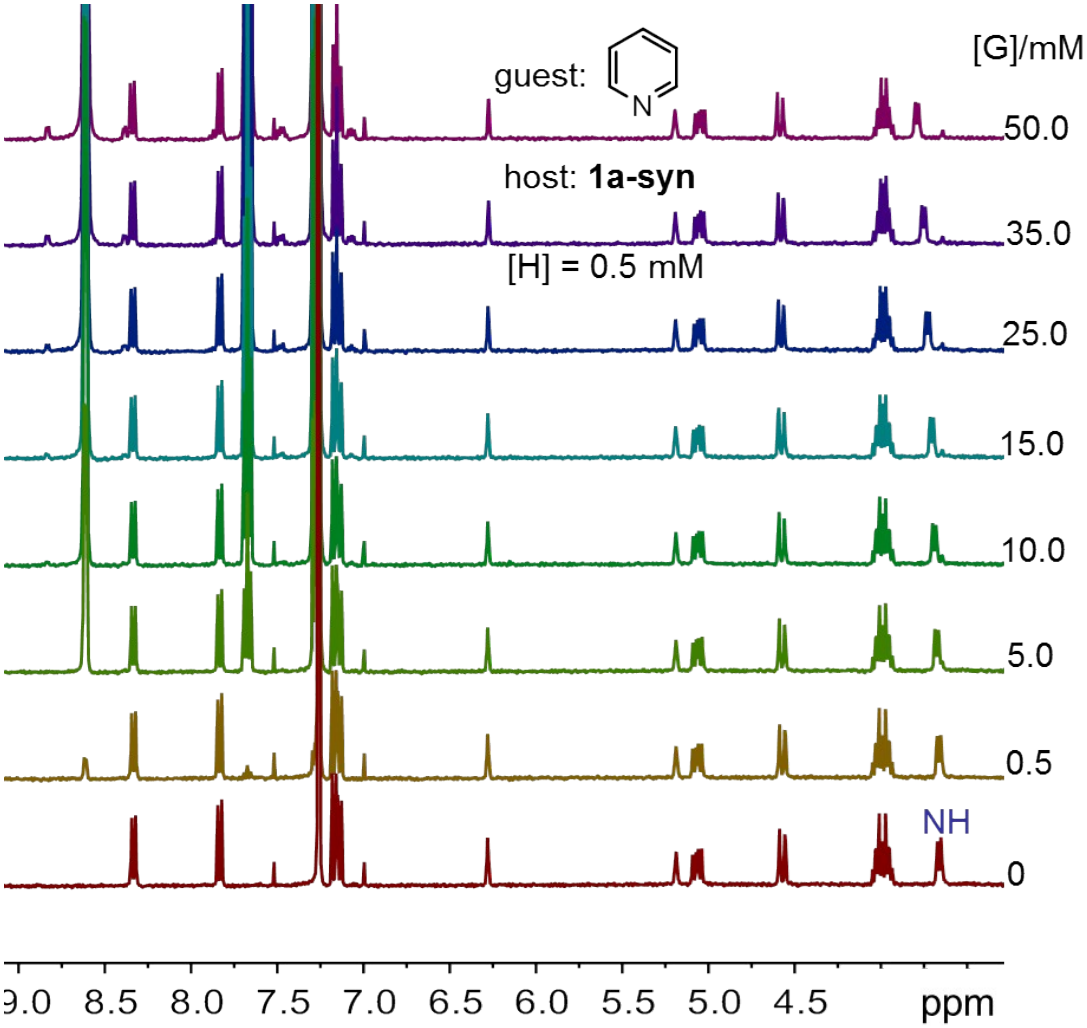

Fig. S57 Partial ^{1}H NMR spectra (400 MHz, $CDCl_3$, 25 ^{o}C) of **1a-syn** (0.5 mM) titrated by the guest **8** (0~50.0 mM). No obvious change on the ^{1}H NMR spectra is observed, suggesting very weak binding between **8** and **1a-syn** (likely < 1 M^{-1}).

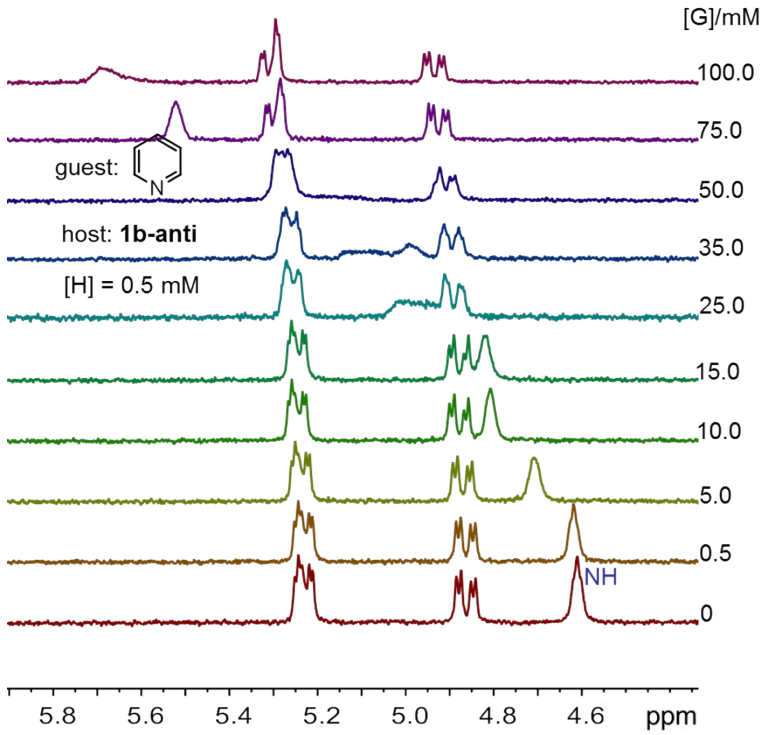

Fig. S58 Partial ^{1}H NMR spectra (400 MHz, $CDCl_3$, 25 ^oC) of **1b-anti** (0.5 mM) titrated by the guest **8** (0~100.0 mM).

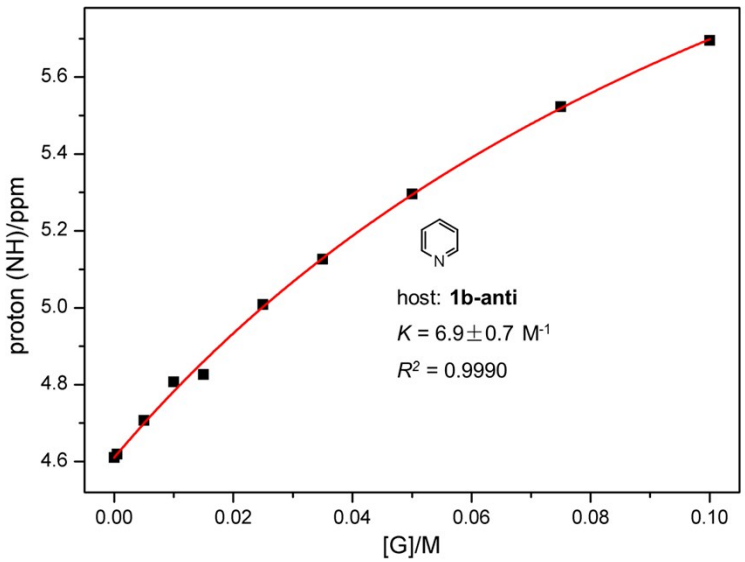

Fig. S59 Non-linear curve-fitting for the complexation between **1b-anti** and the guest **8** in $CDCl_3$ at 25 ^oC.

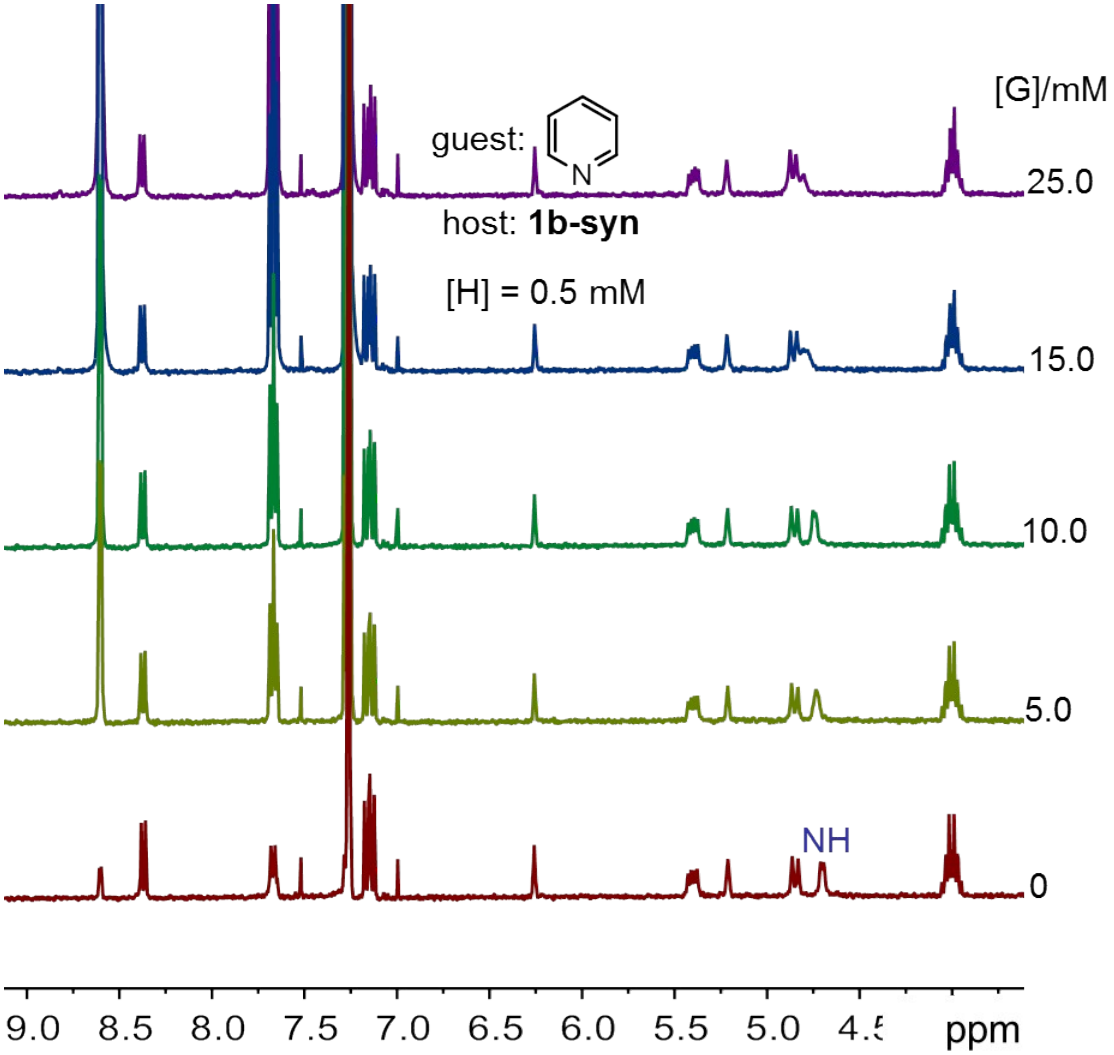

Fig. S60 Partial ^{1}H NMR spectra (400 MHz, $CDCl_3$, 25 ^{o}C) of **1b-syn** (0.5 mM) titrated by the guest **8** (0~25.0 mM). No obvious change on the ^{1}H NMR spectra is observed, suggesting very weak binding between **8** and **1b-syn** (likely < 1 M^{-1}).

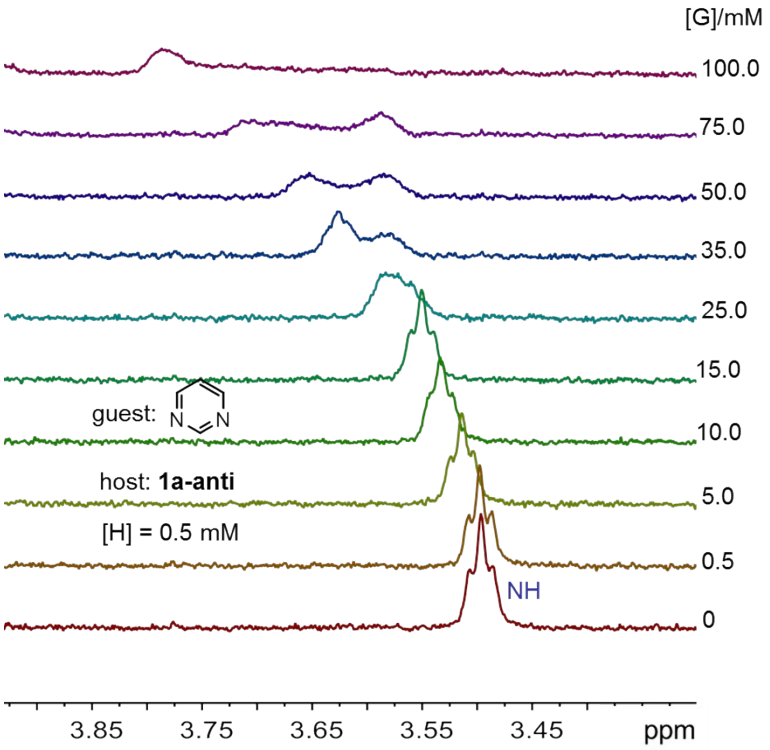

Fig. S61 Partial ^{1}H NMR spectra (400 MHz, $CDCl_3$, 25 ^oC) of **1a-anti** (0.5 mM) titrated by the guest **9** (0~100.0 mM).

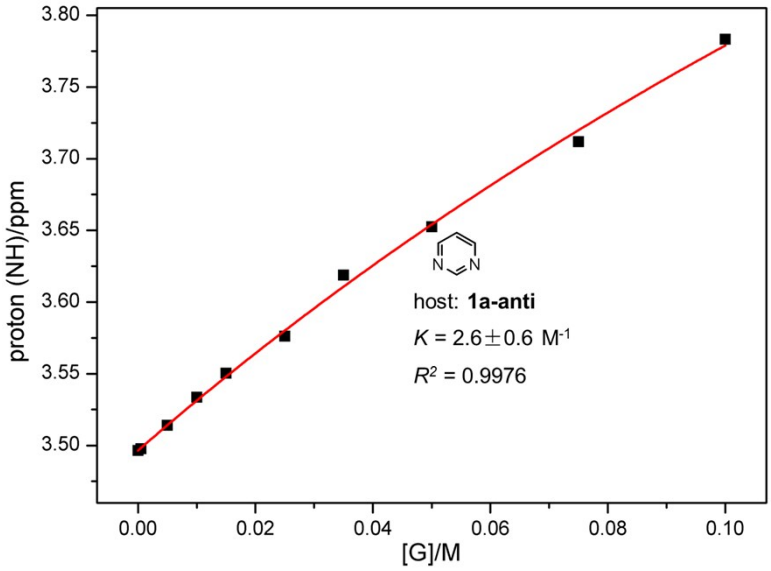

Fig. S62 Non-linear curve-fitting for the complexation between **1a-anti** and the guest **9** in $CDCl_3$ at 25 ^oC.

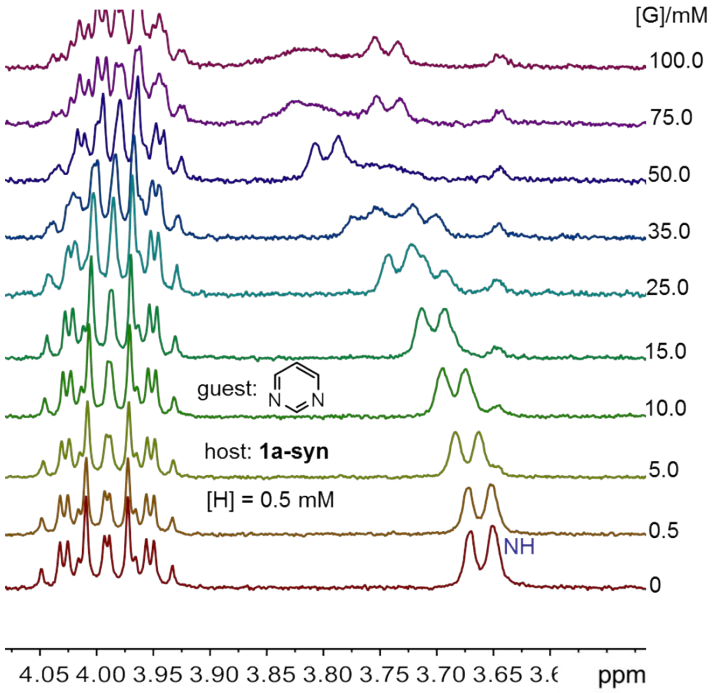

Fig. S63 Partial ^{1}H NMR spectra (400 MHz, $CDCl_3$, 25 ^oC) of **1a-syn** (0.5 mM) titrated by the guest **9** (0~100.0 mM).

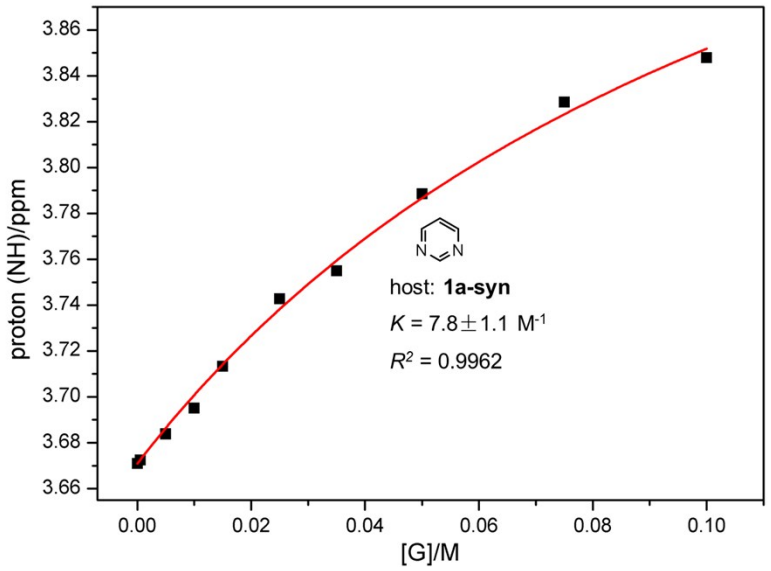

Fig. S64 Non-linear curve-fitting for the complexation between **1a-syn** and the guest **9** in $CDCl_3$ at 25 ^oC.

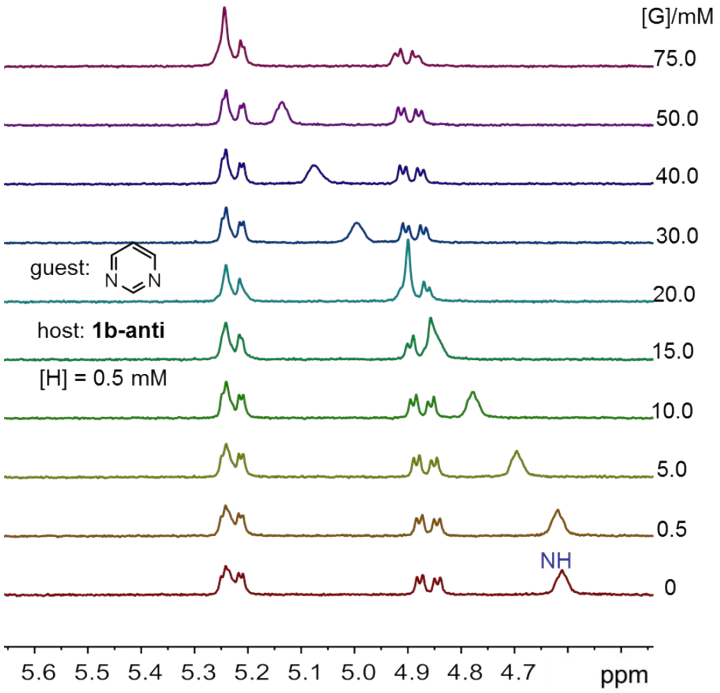

Fig. S65 Partial ^{1}H NMR spectra (400 MHz, $CDCl_3$, 25 ^oC) of **1b-anti** (0.5 mM) titrated by the guest **9** (0~75.0 mM).

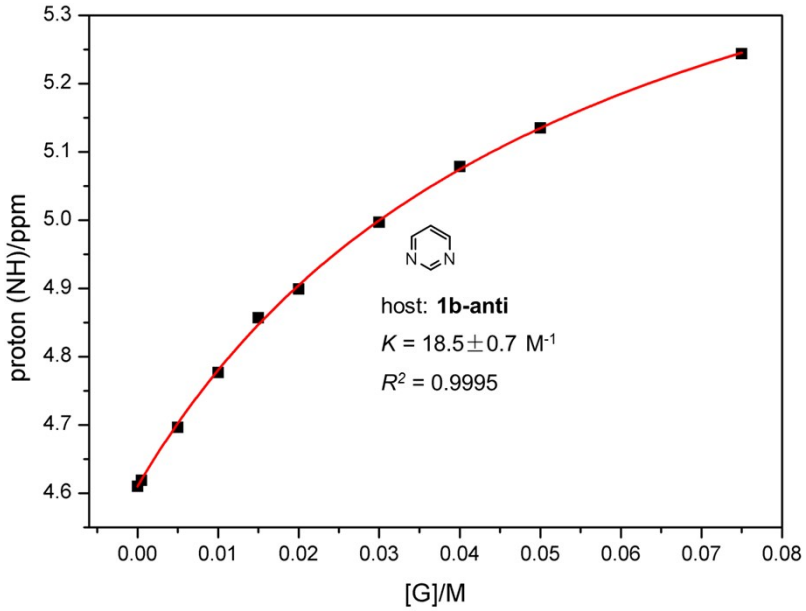

Fig. S66 Non-linear curve-fitting for the complexation between **1b-anti** and the guest **9** in $CDCl_3$ at 25 ^oC.

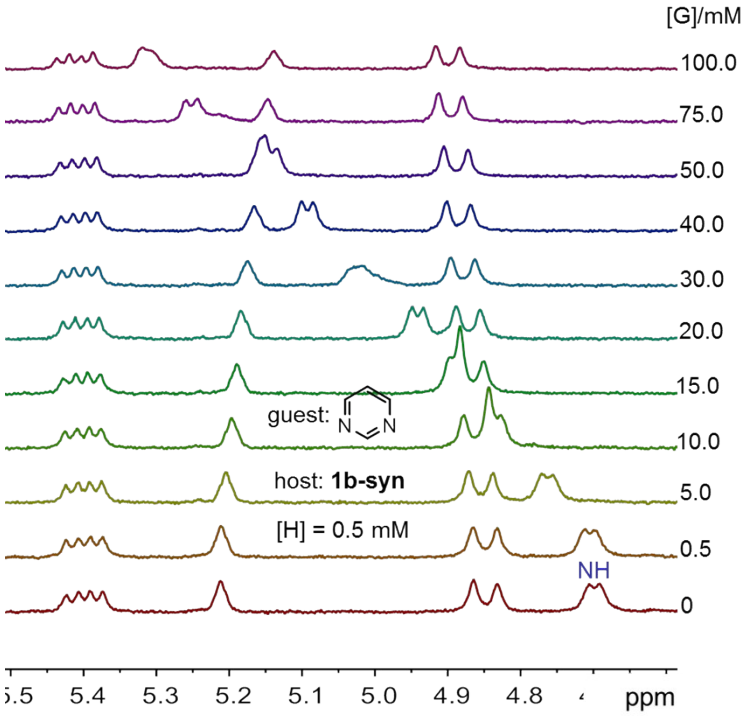

Fig. S67 Partial ^{1}H NMR spectra (400 MHz, $CDCl_3$, 25 ^oC) of **1b-syn** (0.5 mM) titrated by the guest **9** (0~100.0 mM).

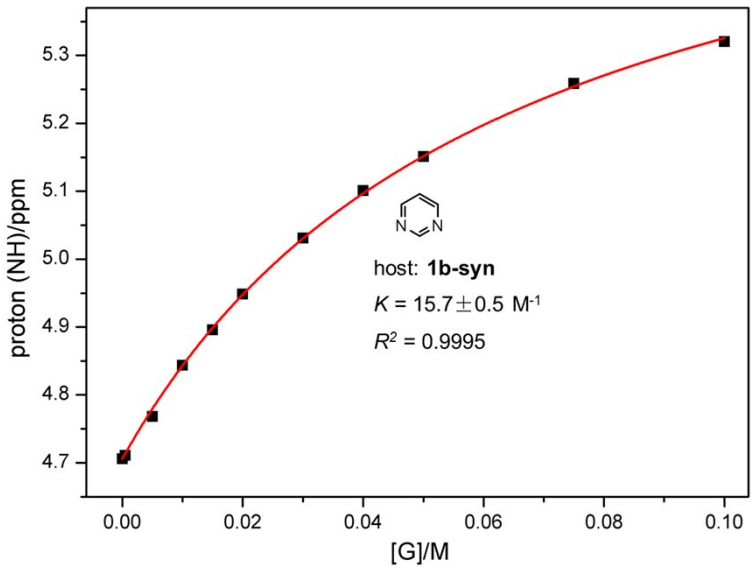

Fig. S68 Non-linear curve-fitting for the complexation between **1b-syn** and the guest **9** in $CDCl_3$ at 25 ^oC.

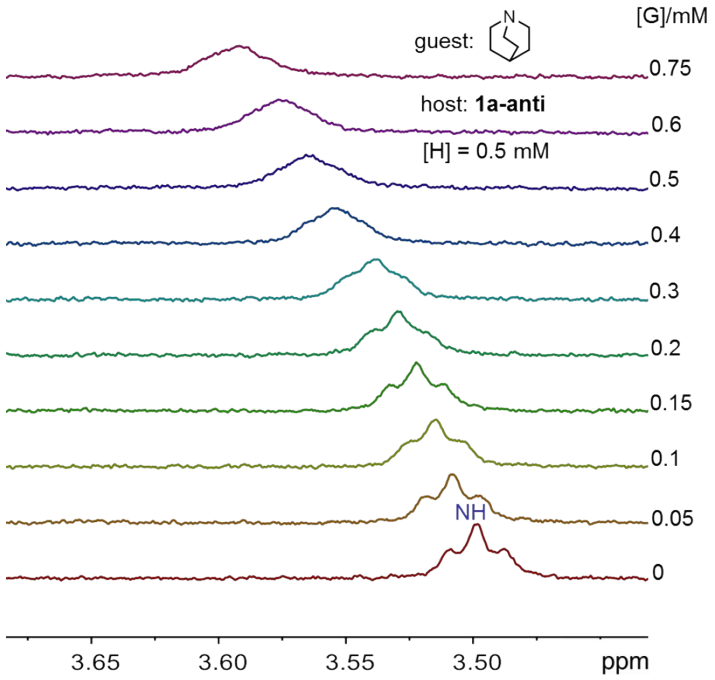

Fig. S69 Partial ^{1}H NMR spectra (400 MHz, $CDCl_3$, 25 ^oC) of **1a-anti** (0.5 mM) titrated by the guest **10** (0~0.75 mM).

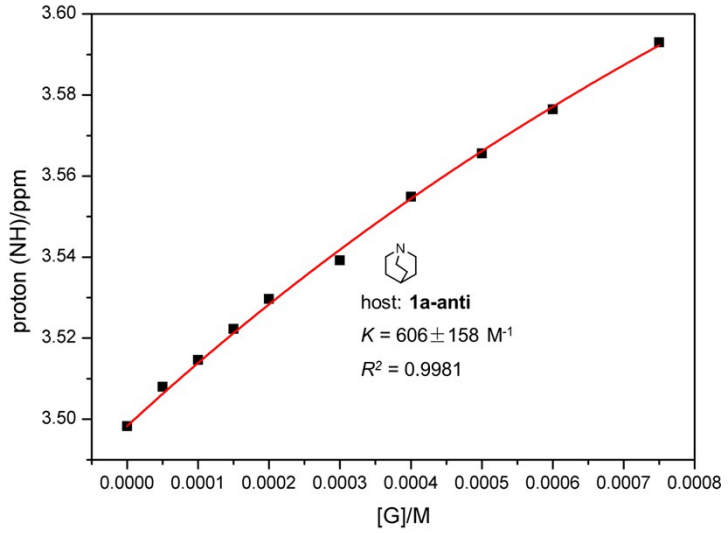

Fig. S70 Non-linear curve-fitting for the complexation between **1a-anti** and the guest **10** in $CDCl_3$ at 25 ^oC.

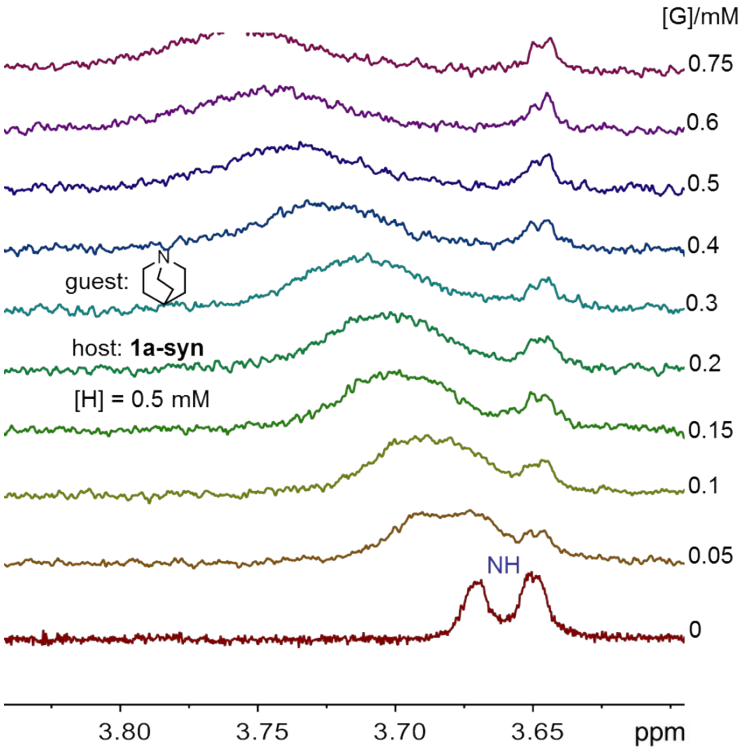

Fig. S71 Partial ^{1}H NMR spectra (400 MHz, $CDCl_3$, 25 ^oC) of **1a-syn** (0.5 mM) titrated by the guest **10** (0~0.75 mM).

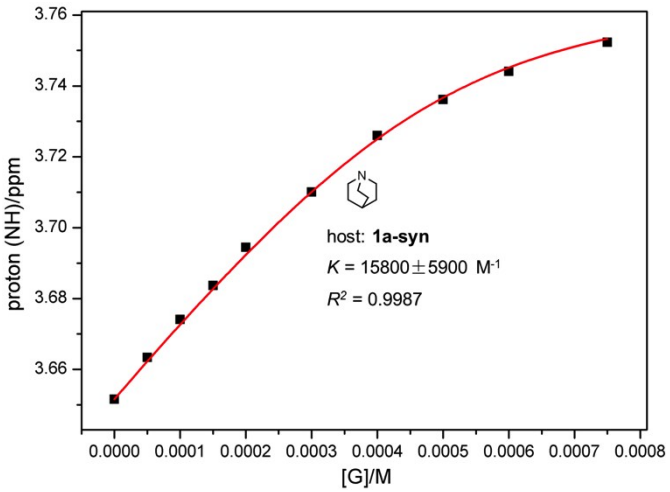

Fig. S72 Non-linear curve-fitting for the complexation between **1a-syn** and the guest **10** in $CDCl_3$ at 25 ^oC.

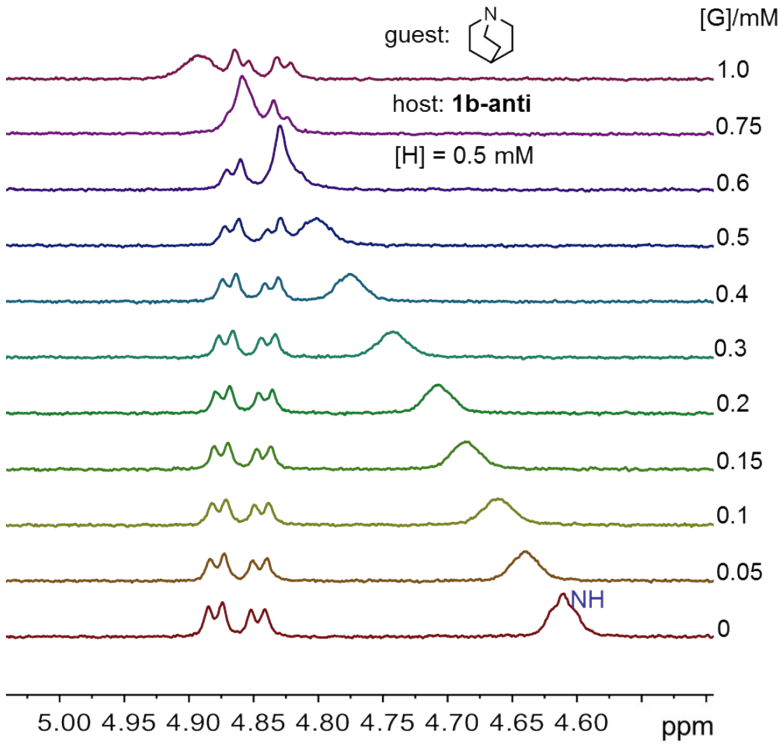

Fig. S73 Partial ^{1}H NMR spectra (400 MHz, $CDCl_3$, 25 ^oC) of **1b-anti** (0.5 mM) titrated by the guest **10** (0~1.0 mM).

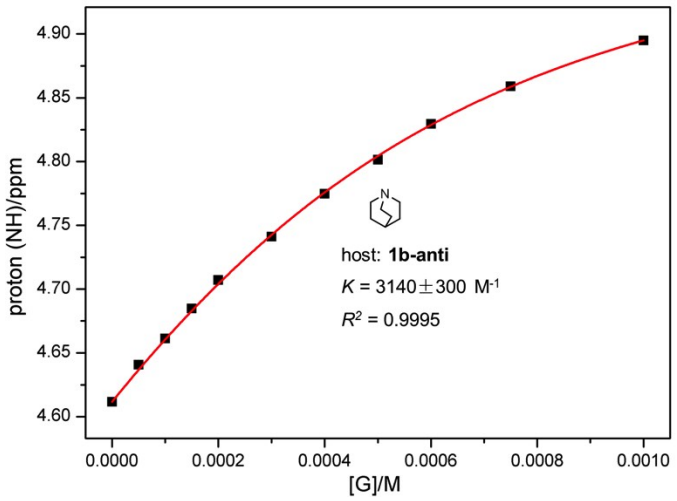

Fig. S74 Non-linear curve-fitting for the complexation between **1b-anti** and the guest **10** in $CDCl_3$ at 25 ^oC.

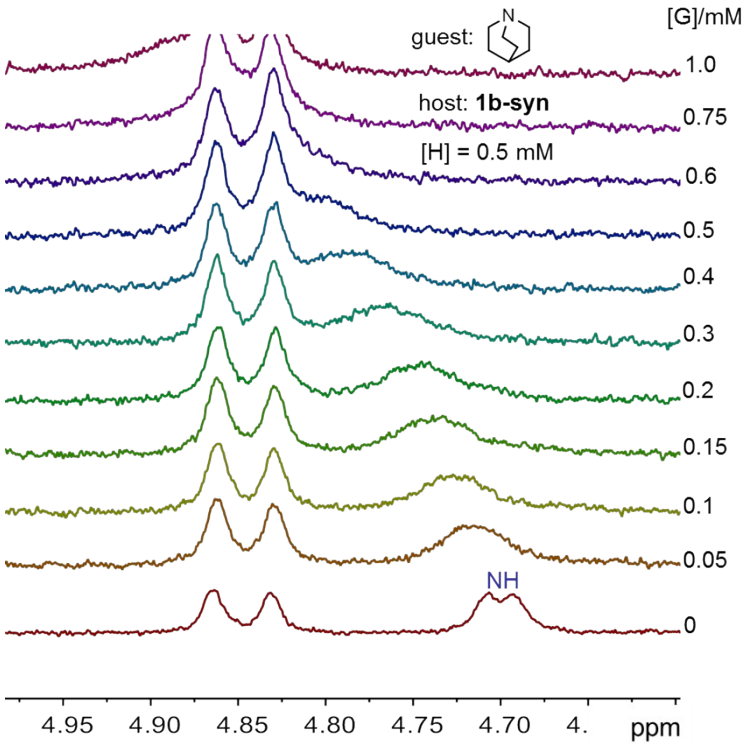

Fig. S75 Partial ^{1}H NMR spectra (400 MHz, $CDCl_3$, 25 ^oC) of **1b-syn** (0.5 mM) titrated by the guest **10** (0~1.0 mM).

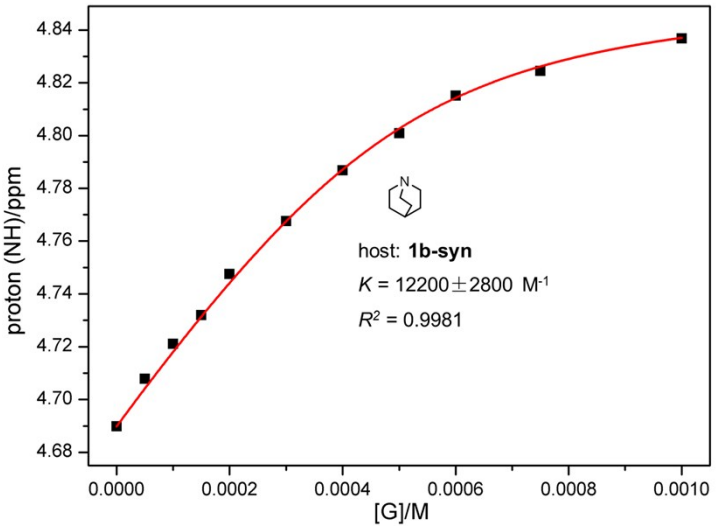

Fig. S76 Non-linear curve-fitting for the complexation between **1b-syn** and the guest **10** in $CDCl_3$ at 25 ^oC.